EPA-650/3-74-007

THE ROLE OF SOLID-GAS INTERACTIONS IN AIR POLLUTION

by

S. Siegel, H. S. Judeikis and C. C. Badcock

The Aerospace Corporation
2350 E. El Segundo Boulevard
El Segundo, California 90245

Grant No. 801340
ROAP No. 21 AJX-3
Program Element No. 1A1008

EPA Project Officer: Jack L. Durham

Chemistry and Physics Laboratory
National Environmental Research Center
Research Triangle Park, North Carolina 27711

Prepared for

OFFICE OF RESEARCH AND DEVELOPMENT
U.S. ENVIRONMENTAL PROTECTION AGENCY
WASHINGTON, D.C. 20460

August 1974

This report has been reviewed by the Environmental Protection Agency and approved for publication. Approval does not signify that the contents necessarily reflect the views and policies of the Agency, nor does mention of trade names or commercial products constitute endorsement or recommendation for use.

ABSTRACT

This study was undertaken to evaluate the potential importance of gas-solid interactions in polluted atmospheres. Model calculations that employed collision theory, transition state theory, and data from the catalysis literature were used to determine the conditions under which the heterogeneous processes could compete with homogeneous gas phase reactions known to be important.

Laboratory experiments were conducted with simulated atmospheres to determine whether or not the theoretically derived criteria could be met under ambient conditions. Among the gases studied were NO_2, NO, O_3, and CO. The selection of the solids used in these studies was based on their abundance in polluted atmospheres, as well as on their known catalytic activity.

Evaluation of the experimental results leads us to conclude that heterogeneous decomposition of NO_2 and O_3, as well as heterogeneous oxidation of CO at ground level, can be important atmospheric processes. Results from experiments conducted in the presence of moisture indicate that water does not poison catalytic activity. In fact, in the case of NO_2, activity is significantly increased in the presence of moisture.

In contrast to the results for NO_2, O_3, and CO, it was found that heterogeneous processes that involve NO are not likely to compete with gas phase reactions.

This report was submitted in fulfillment of Project No. 21AJX-03, Grant No. R801340, by The Aerospace Corporation, under the sponsorship of the Environmental Protection Agency. Work was completed as of October 1973.

CONTENTS

FIGURES

FIGURES (Continued)

TABLES

ACKNOWLEDGMENTS

The authors gratefully acknowledge the efforts of T. B. Stewart, H. R. Hedgpeth, and J. K. Allen in the conduct of laboratory work associated with this program. Appreciation is also extended to M. Birnbaum for use of laboratory equipment, and M. Masaki for performing some of the calculations. We also acknowledge a number of helpful discussions with Jack T. Durham, Chemistry and Physics Laboratory, National Environmental Research Center, Research Triangle Park, North Carolina.

SECTION I

CONCLUSIONS

In the Aerospace investigation of heterogeneous reactions of potential importance in polluted urban atmospheres, significant reaction rates for gas-solid interactions of NO_2, O_3, and CO have been found. In the case of NO, only minimal activities were observed, and we conclude heterogeneous reactions of this species are not likely to be competitive with homogeneous gas phase reactions.

For NO_2, we find significant reaction rates, especially in the presence of moisture, for decomposition on a variety of materials that are likely to be found in polluted atmospheres. These include metal oxides, salts, charcoal, cement, fly ash, and sand. Projection of the laboratory results to the atmosphere, based on the assumption of a total particle loading of $100 \mu g/m^3$, leads us to conclude that the particle limited lifetime for removal of NO_2 would be $\sim$ 1 hr. Although this lifetime is somewhat long compared with the photolytic lifetime ($\sim$ 2-3 min), the homogeneous photo-process does not reduce the total oxidant concentration ($NO_2 + O_3$), as does the heterogeneous process. Thus, NO_2-solid interactions can serve to significantly reduce total oxidant concentrations during daylight hours, as well as lead to an important nighttime sink for NO_2.

Similar reactivities were observed in the case of O_3, as in the case of NO_2, and similar conclusions were reached. However, experiments with O_3 were not nearly as extensive as those with NO_2.

Experiments with CO concentrated on CO-metal oxide interactions. It was found that extrapolation of laboratory results to conservative atmospheric conditions results in significant rates of CO removal at ground level provided that certain minimum rates of regeneration of the metal oxide active sites by atmospheric O_2 are met. The oxides studied were MnO_2, ZnO, CuO, and Fe_2O_3. Using the initial metal oxide activity and atmospheric loadings of 1 g/m^3 (metal oxides only), the lifetime of CO in the atmosphere as a result of the heterogeneous oxidation by atmospheric particles ranged from approximately 606 yr for MnO_2 to 2.6×10^5 yr for Fe_2O_3. Extrapolation of these rates to soils indicate that oxidation by metal compounds on soils could be a significant sink.

SECTION II

RECOMMENDATIONS

It is recommended that these studies be extended to other pollutants, especially SO_2. In the case of CO and O_3, more extensive studies on a wider range of solids are required in order to more accurately estimate the magnitude of possible effects in the atmosphere. Studies should be carried out on solids collected from the environment.

More extensive quantification of the results is needed. This should include estimation of reactivities of the individual components of aerosols and summation of these rates along with those estimated for ground level surfaces. Poisoning and regeneration of the activity of poisoned surfaces should be taken into account. Also, atmospheric mixing and transport phenomena should be considered, along with reactivities to determine whether or not gaseous pollutant gradients exist near ground level surfaces.

SECTION III

INTRODUCTION

NO_x AND O_3

Studies of gas-solid interactions of these species were undertaken to quantitatively determine the extent to which reactions of these air pollutants can be catalyzed on airborne particle or ground level surfaces. [NO_x and O_3 are lumped together here since many of the important reactions leading to disappearance of NO, NO_2, and O_3 originate from the chain initiated by NO_2 photolysis.[1-3] In addition, similar experimental techniques were used in the study of these gases.]

It has been shown by model calculations that under certain favorable conditions, these surface-catalyzed reactions can realistically compete and in some cases dominate the homogeneous gas phase reactions that are usually considered to be important in the atmosphere.[4] This model used a simplified collision model for gas-particle interactions along with transition state theory and experimental activation energies to estimate absorption, desorption, and reaction rates. In general, data from the catalyst literature had to be used. The latter data were usually obtained from experiments conducted at considerably higher temperatures and pressures than are of interest in air pollution studies. Nonetheless, model calculations based on these data suggested the potential importance of gas-solid interactions of NO_x and O_3 in polluted atmospheres. Consequently, a series of experiments conducted under conditions more closely approaching those of polluted atmospheres was deemed desirable. This report describes the results of that experimental program for these gases as well as CO (see below). Experiments were conducted with NO, NO_2, and, to a lesser extent, O_3, using solids representative of those likely to be found in polluted atmospheres. Both dry and moist simulated atmospheres were used. Experimental results were analyzed using appropriate analytical models. Projection to actual environmental conditions was made using the heterogeneous reaction model described elsewhere.[4] The end result of applying these procedures leads us to conclude that particle-catalyzed

decomposition of NO_2 and probably O_3 are likely to be important atmospheric processes. Catalytic oxidation of NO to NO_2 is probably unimportant.

CARBON MONOXIDE

The observed lifetime of carbon monoxide (CO) in the atmosphere has been estimated by Weinstock to be 0.1 yr.[5] Estimates based on the homogeneous gas phase mechanism (Equation 1) yield values of 0.3 to 0.4 yr for the lifetime of CO.[6,7]

$$OH + CO \longrightarrow CO_2 + H \qquad (1)$$

Therefore, a deficit in the observed rate of loss from the atmosphere exists. Several other mechanisms have been proposed[6] ranging from sea water adsorption and bacterial degradation in soils to stratospheric reactions. Almost without exception the oxidation of CO by airborne metal oxide particles has been excluded. This is probably due to the lack of studies in the area and to the conclusion of Nagarjunian and Calvert[8] that metal oxide oxidation of CO was an unimportant sink. Their studies were based on a single metal oxide (ZnO) under photo-oxidation conditions.

A review of the literature shows that very few heterogeneous oxidation studies of CO over metal oxides have been done under conditions that can be extrapolated to the atmosphere. Most studies have been performed at high temperatures under high CO loadings. Another problem with most studies is that they have been done under equilibrium conditions, that is, the rates of reaction are those determined at high CO concentrations some time after the reaction has been initiated.[8,9] First, since ambient CO concentrations seldom exceed 10 ppm even in polluted atmospheres, these conditions may not apply. In addition, the ratio of CO to oxygen is generally less than 5×10^{-5}, thus the regeneration of reactive sites could be favored by such concentration differences in the atmosphere.

For the heterogeneous oxidation of carbon monoxide to be an important contributor to the CO sink in the atmosphere, the rate of reaction must exceed certain values. Generally, the equilibrium rates given in the literature are too slow,[8] however consideration of a simple heterogeneous mechanism can demonstrate how an initial rate can be much greater. Consider a metal

oxide (M_xO_y) with an initial concentration of active sites of different types and reactivities A, B, C .... Then the oxidation of CO at the various sites and the regeneration of the sites can be described by the following reactions.

$$CO + M_xO_y(A) \rightarrow CO_2 + M_xO_y(B) \quad (2)$$

$$CO + M_xO_y(B) \rightarrow CO_2 + M_xO_y(C) \quad (3)$$

$$O_2 + M_xO_y(C) \rightarrow M_xO_y(B) \quad (4)$$

$$O_2 + M_xO_y(B) \rightarrow M_xO_y(A) \quad (5)$$

If the concentration of the A type sites is low but their reactivity is high and the opposite is true for the B type sites, an experimental study of the oxidation would yield data only for the B type sites at high CO pressures. Furthermore, the regeneration reactions (which would result in catalytic activity) could be too slow to form enough A type sites to provide more than a small effect on the overall rate of production of CO_2 as long as the ratio of CO to O_2 was large. Kobayashi and Kobayashi have published a series of papers describing a mechanism for the CO oxidation over manganese dioxide (MnO_2) which is similar to that outlined above.[10-12]

Nearly any experimental method chosen to study the initial behavior of a metal oxide during heterogeneous oxidations runs the risk of integrating out that data which might be most pertinent to an atmospheric study. First the minimum detectable limits may require collection of such a relatively large sample of product that the initial rate is not detected. Second, metal oxides can return CO_2 either irreversibly or reversibly with a slow rate of desorption.[9-12] This again can result in failure to determine the initial rate of CO_2 production. We have chosen the slug-type micro-reactor[13] with product collection to study the heterogeneous oxidation of CO over several metal oxides. This technique results in high sensitivity and can overcome the problem of slow desorption.

The results from experiments conducted with this system leads us to conclude that heterogeneous oxidation of CO on metal oxide particles in the atmosphere is probably not an important process, however, a similar process on ground level surfaces would be significant.

SECTION IV

DESIGN AND EQUIPMENT FABRICATION

GENERAL

Four different reactor systems were used in these studies. Two of these systems were cylindrical flow reactors that differed from each other primarily in their method of reactant/product detection. Optical absorption using a chopped dual-beam system was utilized in one reactor, whereas, detection of laser-induced fluorescence was used in the other. These will be referred to as the CFA (cylindrical flow-absorption) and CFF (cylindrical flow-fluorescence) reactors, respectively. The CFA reactor was used in studies on NO_x and O_3, and the CFF reactor was used to investigate heterogeneous decomposition of NO_2. The third system was a pulsed microcatalytic reactor (designated the PMC reactor) that was used in the study of catalytic oxidation of CO. The fourth was a bulk reactor used for preliminary experiments with CO.

CFA REACTOR

Reaction Chamber

The reaction chamber was made from 50-mm-i.d. pyrex tubing with 30-mm-dia pyrex windows fused on the ends that were tapered to accommodate the pyrex windows. Single 6.6-mm tubes were fused onto the cylinder walls at either end to provide for input and exit of the reacting gas mixture. The ends of the reactor were tapered over a distance of about 30 to 35 mm to reduce flow related problems. The reaction chamber was constructed in two parts with an O-ring joint near the exit to provide access for loading the catalysts.

Surrounding the reaction chamber were eight F15T8D daylite fluorescent lamps. The chamber and lamps were enclosed in a 13-cm-dia chrome plated cylinder, which acted as a reflector. The lamps were independent from one another and each couid be operated at the normal current of 0.300 A (15 W) or in a high power mode at 0.600 A by switching in either a single ballast or two ballasts in parallel. The daylite fluorescent lamps have a spectral distribution

nearly equivalent to sea level sunlight (Figure 1) with a maximum intensity of 3.2 ± 0.5 times the average sea level intensity.

With all fluorescent lamps operating at high power, a black catalyst will absorb enough energy to raise its temperature only 5 °C. Cooling for the lamps themselves is provided by a 2800-l/min squirrel cage blower pulling air through the 13-cm-dia chrome cylinder.

In some experiments a 1-mil-thick layer of DuPont Kapton^{R} was wrapped around the outside of the reaction chamber in order to prevent photodissociation of NO_2. The transmission characteristics of this filter are also illustrated in Figure 1. At 410 nm (worst case) this filter transmits about 0.15% and the quantum yield for photodissociation[14] is about 0.2. With the use of this filter, gas phase NO_2 dissociation was not detected.

Catalysts were introduced into the chamber by supporting them on the surface of either a glass helix or a solid glass cylinder. The helices were made from 3-mm-o.d. pyrex rod by winding 77 turns on a 32-mm-dia mandrel. Thus the helix was shaped like a cylinder with an inside diameter of 3 cm and a length of 43 cm. The spacing between the coils was about 3 mm. The helix was used for photolytic experiments. The solid glass cylinder had an inside diameter of 40 mm and a length of 400 mm. The cylinder and helix were placed in the chamber such that they were coaxial with the reaction chamber.

Gas Handling System

Gas flows are illustrated schematically in Figure 2. There are two Matheson Company model 660 gas mixers for mixing Matheson nitrogen oxide-nitrogen or argon mixtures with diluent nitrogen or argon and for mixing this resultant mixture with Matheson ultra-high purity oxygen. At the ends of the chamber, there are Nupro cross pattern needle valves for sampling entrance and exit gas streams. The outputs from these valves are fed to a four-way teflon stopcock such that one stream is directed to the chemiluminescent monitor for NO (CLEM) and the other stream goes to the mass spectrometer sampling valve and then to the gas chromatograph sampling valve. The Brooks R-215-D flow meter at the chamber exit measures the total flow through the chamber and is the only flow meter which

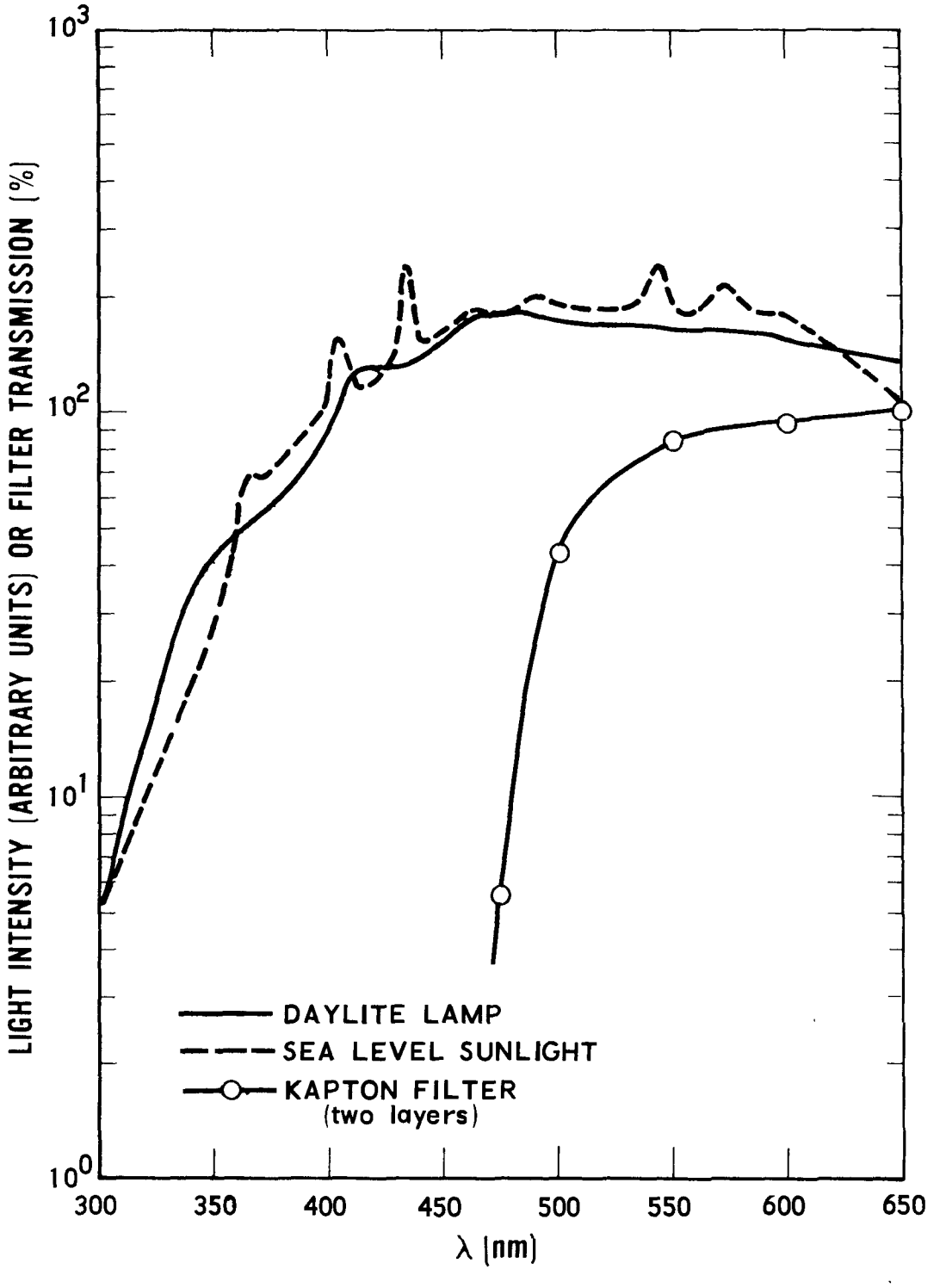

Figure 1. Experimental light intensities and filter transmission compared to the sea level solar spectrum

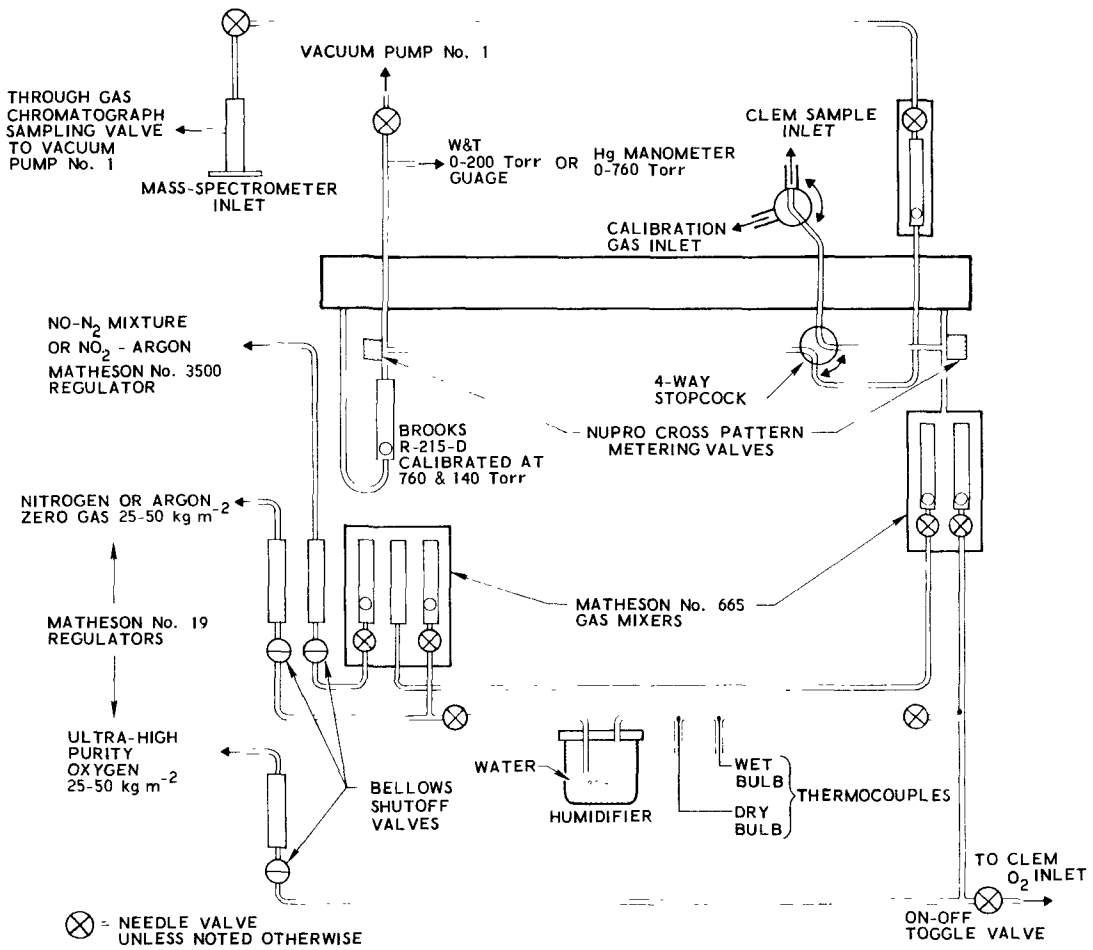

Figure 2. Gas flow system

has been calibrated against a wet-test meter.

Humidifier

For experiments conducted as a function of relative humidity, a separate gas stream must be humidified and mixed with the NO_x-N_2 or argon mixture prior to entering the catalytic chamber. The fact that NO_x is soluble in and somewhat reactive with H_2O prevents the direct humidification of the gas mixture. Humidification was accomplished by bubbling an inert gas such as argon or nitrogen through a gas washing bottle and mixing with the NO_2. The humidity of the NO_x gas mixture can be regulated by controlling the water temperature in the humidifier and the amount of humidified gas that is mixed with the NO_x gas mixture. The moisture content of the reacting mixture was measured by the temperature difference between a dry and wet bulb copper-constantan thermocouple combination.

Gas Analyzing System

Chemiluminescent Monitor (CLEM) - The chemiluminescent monitor for NO illustrated in Figure 3 utilizes the chemiluminescent reaction between ozone and nitric oxide to monitor either nitric oxide or ozone concentrations.[15] For these experiments, however, only the nitric oxide concentrations were monitored. The ozone used for the reactions was made from oxygen at 200 Torr in a silent discharge. The oxygen flows between concentric thin wall (1 mm) pyrex cylinders spaced 1 mm apart. Copper sulfate solution is used as electrodes, and a potential of 4000 V ac is applied between the inside and outside cylinders. At the given operating conditions, ~ 4 Torr of ozone is generated or about 2% conversion.

The analysis takes place when the ozone-enriched oxygen is mixed with a sample of entrance or exit gas from the main reaction chamber. The mixing takes place inside a 1-liter spherical pyrex flask that has been painted white on the outside. A United Technology PIN-25 photodiode with a red filter is mounted near the top of the flask to monitor the chemiluminescent reaction.

Calibration of the CLEM is accomplished by supplying either 1,000 or 10,000 ppm (± 2%) nitric oxide diluted with nitrogen in place of the chamber gas. Because of the dc drift in the photodiode-electrometer system, the

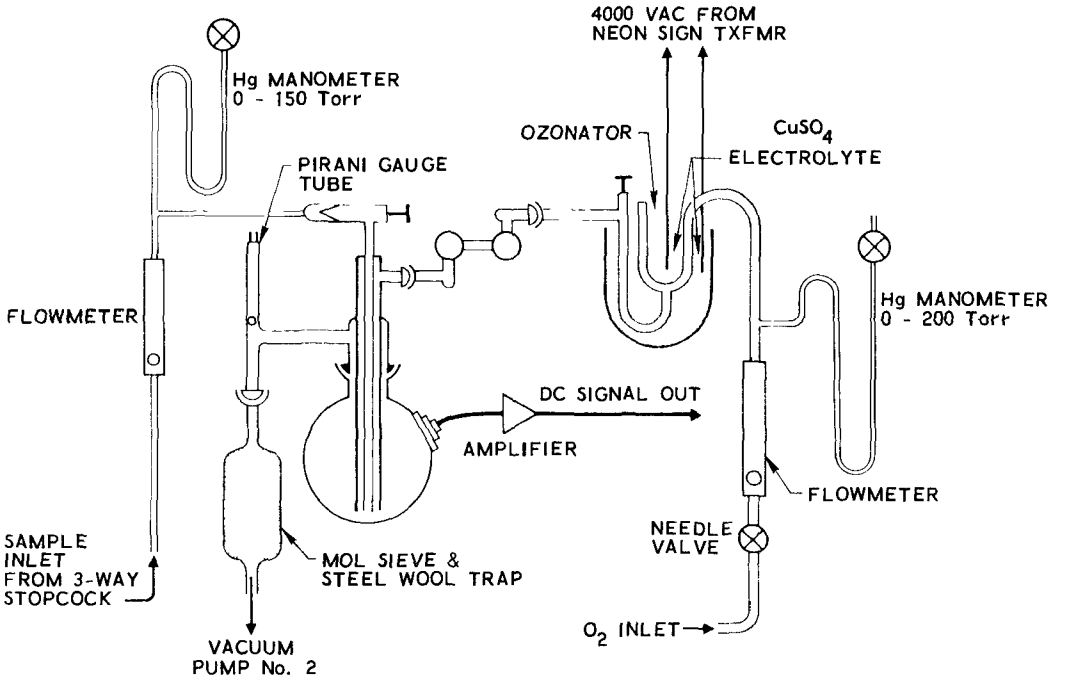

Figure 3. Chemiluminescent monitor for NO

minimum sensitivity is about 50 ppm NO; the response is linear to at least 10,000 ppm NO. A 2,000 ppm nitrogen dioxide-nitrogen mixture gives no detectable signal.

Gas Chromatograph and Mass Spectrometer - The gas chromatograph is an F and M (Hewlett-Packard) model 810 equipped with a Carle 2114 sampling valve, thermal conductivity detectors, and a stable dc amplifier. The column used for nitrogen-oxygen ratio determinations is a 6.6-mm-dia aluminum column of Linde molecular sieve 5A, 60 to 80 mesh (with fine particles removed), 2-m in length, and is activated periodically at about 300° C. For low noise, the bridge current was supplied by two 6-V dry-cell batteries connected in series.

The quadrupole mass spectrometer is an E. A. I. Quad 200 pumped by a 100 l/sec ion pump. The gas can be analyzed by inletting the gas through a leak valve modified to sample a flowing gas stream with little stagnation. This instrument was not used on oxides of nitrogen because the nitrogen dioxide dissociates. It was included in the system for use on other gases.

Optical System - The average NO_2 concentration in the reaction chamber is determined by photometric absorption. The dual-beam system is illustrated in Figure 4. The light source is a fan-cooled 450-W tungsten filament sun gun lamp with quartz envelope. A 5-cm water filter with a 475-nm narrow band interference filter and Corning 3-72 yellow filter is placed in the optical path.

A fraction of the light is passed through a pinhole and lens to a 90 deg mirrored face, chopper blade that rotates at 11.3 Hz on an inclined axis of 45 deg to the incident light beam. At one phase of the chopper, the light passes through the open sections of the chopper blade and through another lens into the reaction chamber, through the chamber and is reflected off an (adjustable) first surface mirror into the integrating sphere. At the other chopper phase, the light is made to by-pass the chamber by reflecting off one of the two front surface mirrors on the chopper blade through a series of lenses and mirrors into the integrating sphere. The two beams are combined orthogonally at the integrating sphere, which is coupled (orthogonally) through another 475-nm narrow band interference filter to a 1P21 photo-

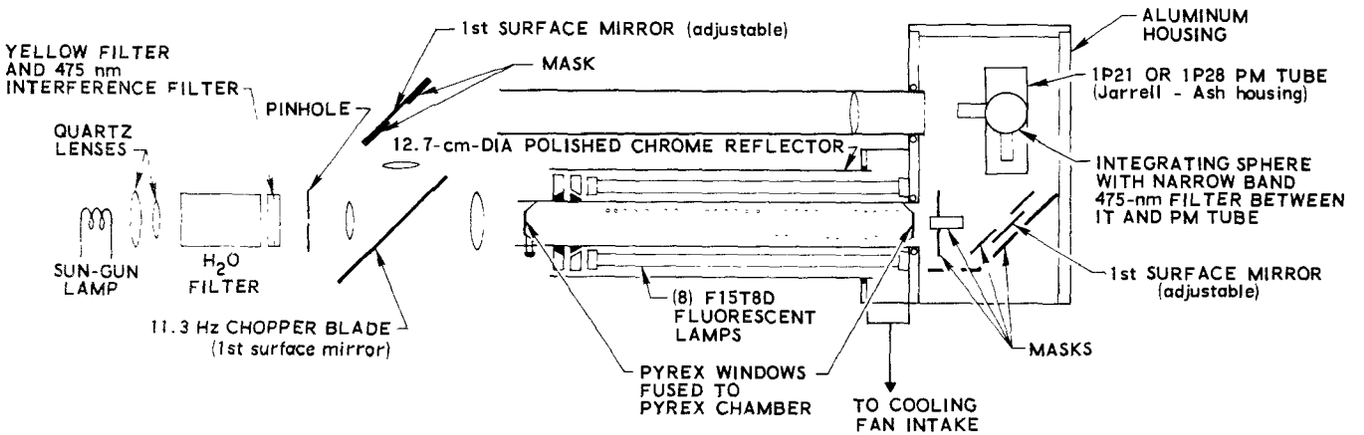

Figure 4. Optical system (CFA reactor)

multiplier tube operated at -1000 V.

The photomultiplier tube output is fed to a Brower model 129 thermocouple amplifier (lock-in voltmeter). The baseline drift of the system is about one part per thousand short term (10 min) and about five parts per thousand overnight. An intensity change of one part per thousand (O. D. 0.0004) corresponds to about 1.5-m Torr NO_2 in the chamber.

The absorption spectrum of NO_2 is quite structured.[16] This fact, coupled with a filter bandpass of about 10-nm, required that an average extinction coefficient (ϵ) be determined. This average was determined by use of a Cary-15 uv/visible spectrophotometer and a 2.5-cm gas cell. The absorption spectrum of NO_2 and the filter are illustrated in Figure 5. The filter and empty gas cell were measured in the spectrophotometer and the spectrum was integrated to give I_o. Similarly the filter and gas cell with a low pressure of NO_2 was measured and integrated to give I. The values of I_o, I, path length, and NO_2 pressure (corrected for N_2O_4 content) were substituted into the Beer-Lambert law; the average value of ϵ calculated was 98 $l\text{-mol}^{-1}\text{-cm}^{-1}$.

CFF REACTOR

The fluorescence apparatus used for the experiment is shown in Figure 6. This system, which was constructed under the direction of Dr. M. Birnbaum, was initially used to measure, on a real-time basis, the atmospheric concentration of the oxides of nitrogen.[17] The apparatus is a vacuum chamber capable of obtaining pressures of 10^{-4} Torr. The laser light from a Spectra Physics model 140 argon ion laser enters the vacuum chamber through a 4880 interface fiber, iris diaphragm, and a series of light baffles. The light then enters the observation chamber where the NO_2 fluorescence excited by the laser beam is transmitted, at right angles to the exciting light, through a series of optical filters and focused by a 75-mm focal length lens on an EMI 9659 QAM photomultiplier tube. The signal is monitored on a pulse counter and displayed numerically. The system was slightly modified to accommodate our flow reactor experiments. The air sampling inlet was replaced by a gas bottle containing 2000 ppm NO_2 in argon and a Matheson 603

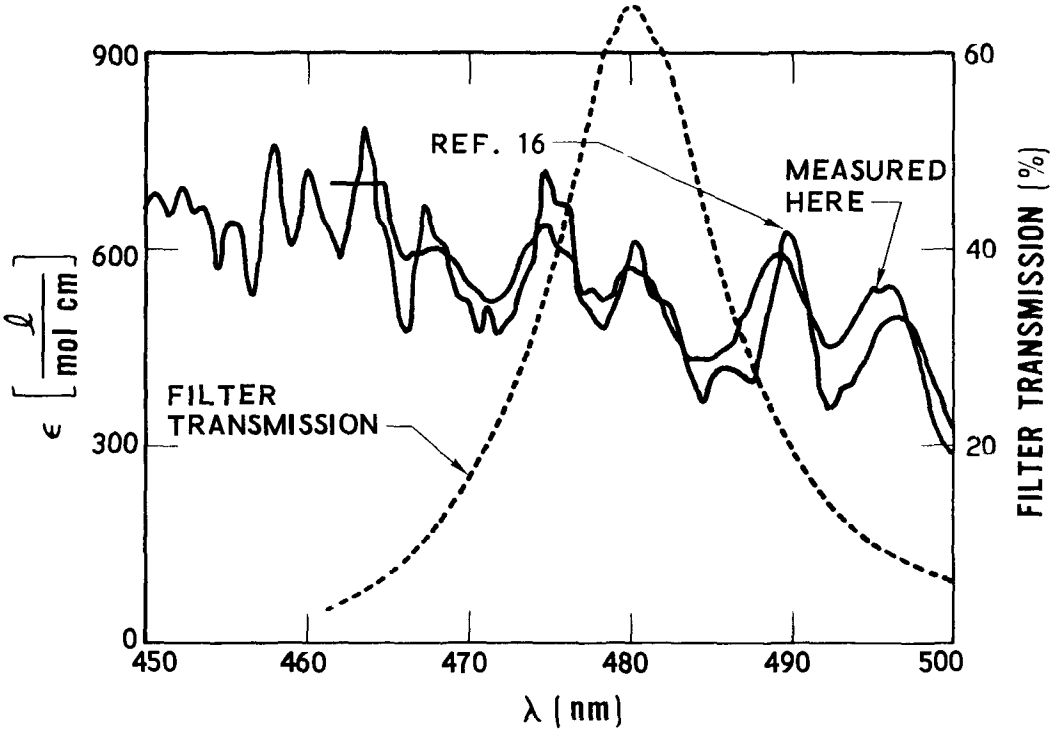

Figure 5. Absorption spectrum of NO_2 and filter transmission

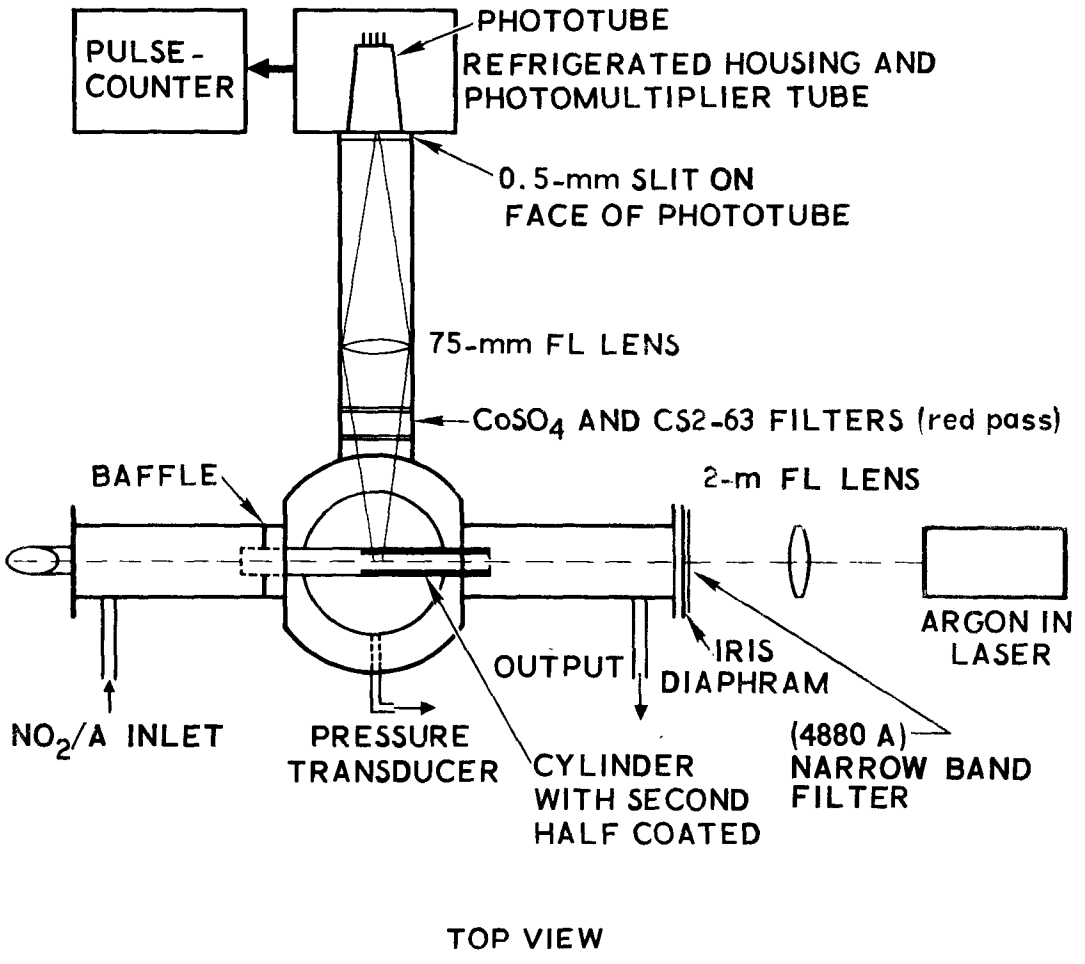

Figure 6. Diagram of CFF reactor

flow meter which was calibrated over a pressure range of 1 to 100 Torr. A Dynascience model P70 pressure transducer was added to monitor the total pressure with a sensitivity of 10μm. Light baffles were removed so that the chamber could accommodate the cylinder. Baffles were placed on the cylinder ends to reduce scattered light. The sensitivity for detecting NO_2 was 10^{-2} Torr.

The spatial resolution of 0.5 mm was achieved by using the 75-mm lens and 0.5-mm slit in combination. The slit was placed on the face of the photomultiplier tube which was located at an image distance of 150 mm from the lens. This image distance was exactly the same as the object distance of the laser beam from the lens. Thus, by placing the slit on the photomultiplier and using the image and object distance relationship with a thin lens, one gets a magnification of one, thus a spatial distance on the beam of 0.5 mm.

For most of the catalytic measurements, a 1-cm radius pyrex cylinder was placed in the chamber on a movable platform in such a way that the cylinder axis coincided with the laser beam. The movable platform, shown in Figure 7, was constructed from a precision dovetail slide to which was attached a 32 pitch rack. The rack was used in combination with a 32 pitch spur gear mounted on a rotating shaft. This gear combination gave no backlash motion when the platform was moved back and forth. Linear motion was imparted to the slide from outside the fluorescence chamber by rotating the shaft that passed through an ultra-Torr vacuum fitting. The vacuum fitting was attached to the vacuum flange and a leak-tight seal was made by pressing a viton O-ring against the shaft. No leaks were detected at 10^{-4} Torr pressure when the shaft was rotated. A pointer affixed to the shaft indicates the position of slide by virtue of it pointing to a scale in the flange. The position of the slide could be measured to 0.25 mm. By using larger pitch gears and larger radius scales, better accuracy in position could be measured. The total linear displacement of the platform was 45 mm.

PMC REACTOR

General Description

The experimental design of the system is a modified version of the micro-

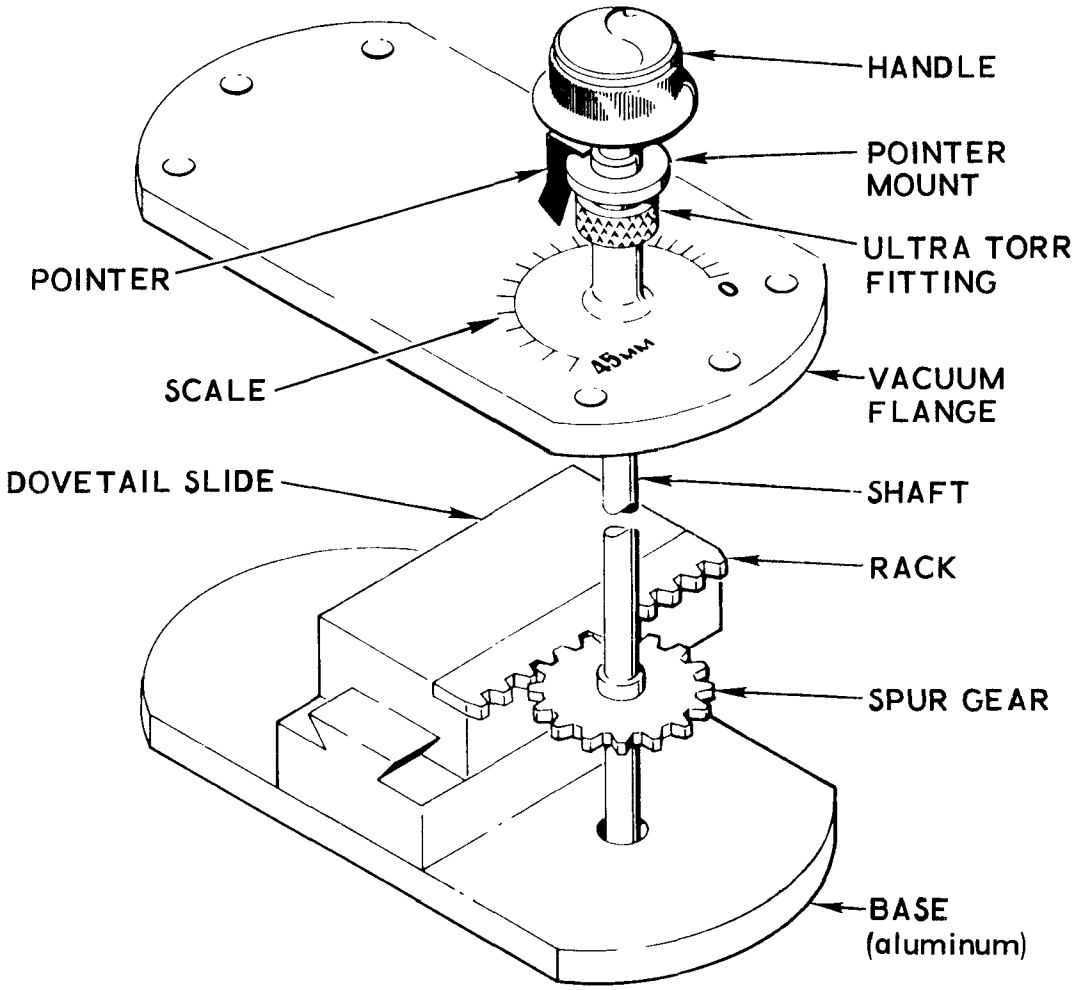

Figure 7. Movable platform used in CFF reactor

catalytic slug reactor originally described by Hall and Emmett.[13,18] It consists of a vacuum line for measuring and mixing gases, a gas sampling valve that is used to introduce slugs of the gas mixture into a reactor via the helium carrier gas, a CO_2 collection loop, and a gas chromatograph for qualitative and quantitative analysis of the reactants and products. A flow diagram of the experimental apparatus is shown in Figure 8.

Gas Mixing System

The gas mixing system is a glass high vacuum line using Kontes teflon O-ring stopcocks, a hand operated piston type pump for mixing gases,[19] two precalibrated bulbs of different volumes for calibration and measuring, a Matheson 0 - 760 Torr vacuum gauge, and a Validyne pressure transducer with exciter-demodulator and VOM for pressure measurements in the low pressure region. The pressure transducer, vacuum gauges, and parts of the gas chromatograph are connected with metal Swagelok connectors. The connectors between the gas chromatograph and vacuum system are via flexible metal to glass seals.

Slug Reactor and Gas Chromatograph

The reactor and chromatograph consist of a series of gas sampling valves and calibrated loops that are followed by two chromatographic columns and a thermal conductivity detector. A small sample of the gas mixture from the gas mixing system is drawn into a previously evacuated sample loop (0.5 cc) in a Carle, eight port, two-position gas sampling valve (GSV). The Carle GSV was fitted with plates top and bottom and purged with helium to prevent air leakage. When this sample is switched into the helium carrier stream, it passes through the reference side of a Carle micro volume thermistor thermal conductivity detector and then into a Loenco six port GSV. The Loenco GSV is arranged such that the sample may by-pass or be admitted to the reactor loop containing the suspended metal oxide. This valve also allows connection of the reactor loop to the vacuum system to allow for activation (when in the by-pass position). The gas flow then enters a Whitey four-way ball valve where the flow may either be directed through a stainless steel loop or by-pass it. The loop may be cooled with liquid N_2 for collection

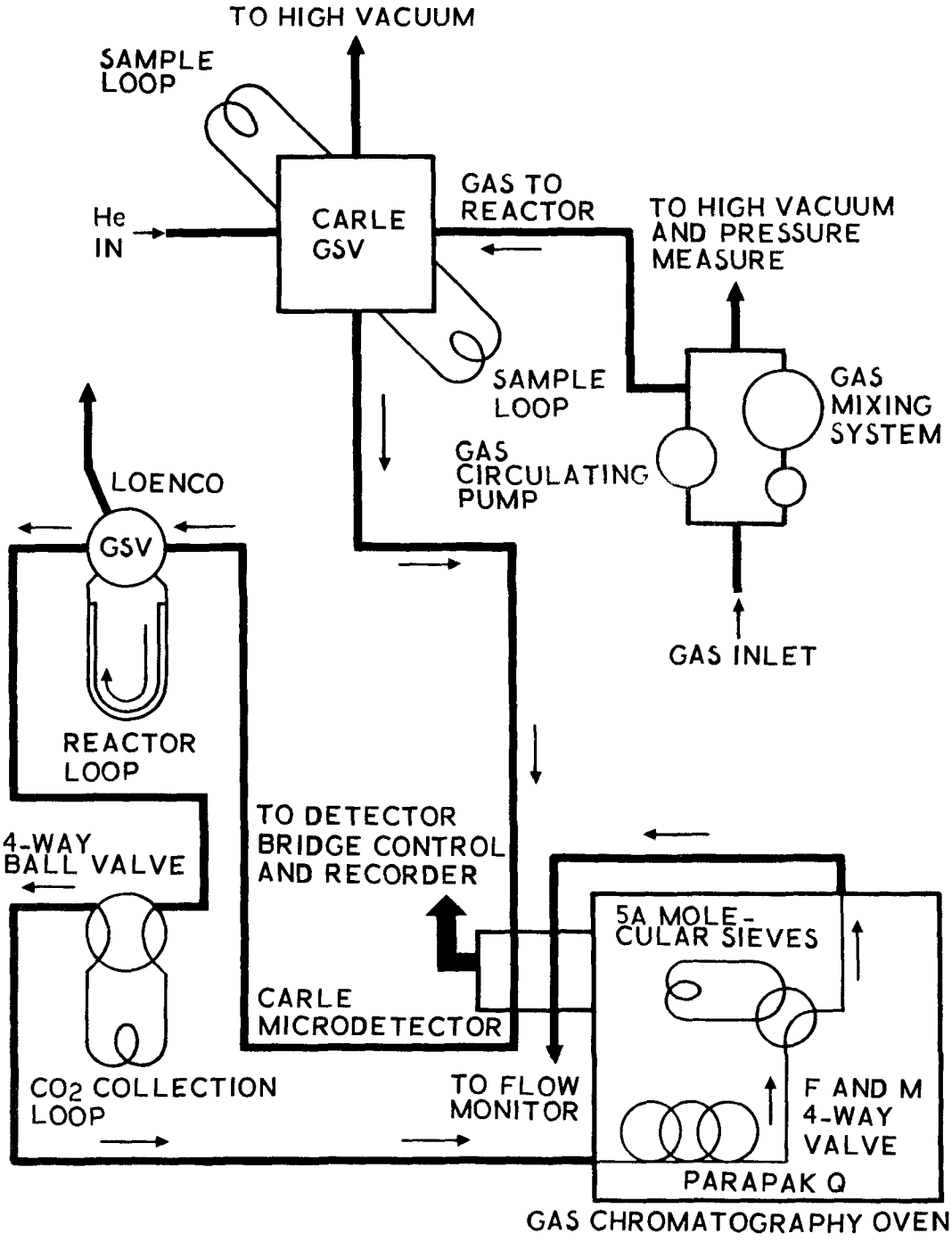

Figure 8. Slug reactor system

of the product CO_2. The gas stream then enters the gas chromatographic section.

The gas chromatograph is a modified Loenco blood gas analyzer (AD 2000) oven coupled with the detector described above. The chromatographic columns are a 1.8-m by 0.32-cm (O.D.) Porapak Q column that is connected to an F and M four-way valve that switches in or by-passes a 7.6-cm by 0.64-cm (O.D.) molecular sieve 5A column. The effluent then enters the sample side of the detector and exits through a ball-type flow meter. The Porapak Q column resolves CO and O_2 from CO_2; the molecular sieve column resolves the former two components and N_2. The detector is powered by a Carle 100 micro detector control, and the data is displayed on a Leeds and Northrup strip chart recorder running at 2 in min^{-1}.

Materials

Manganese dioxide and cupric oxide were obtained 99% pure from ROC/RIC Research Chemical. Ferric oxide used was commerical jewelers rouge, and zinc oxide was obtained from the New Jersey Zinc Company. All were used as received. Surface areas by the BET method[20,21] for the metal oxides were MnO_2 - 97 m^2/g, ZnO - 22.2 m^2/g, Fe_2O_3 - 27.3 m^2/g, and CuO - (5) m^2/g. The support material for the metal oxide in the catalyst loops was 90/600 mesh Tee-Six, a Teflon Six powder from Analabs. Helium from Air Products was passed through a molecular sieve 5A trap at -196 °C (L-N_2) to eliminate CO_2 and water from the carrier gas. Helium to purge the Carle GSV was used as supplied. Matheson C.P. carbon monoxide and extra dry oxygen were passed through a -78 °C silica gel trap to remove CO_2 and H_2O. Carbon dioxide used in peak-area calibrations was obtained from dry ice and pumped on at -78° and -196 °C to remove air.

Reactor Loops

The reactor loops were U-shaped, 21 - 24-cm long pyrex glass tubes, 6-cm O.D., and were attached to the Loenco GSV by Swagelok nuts and Viton O-rings. The metal oxide and Tee-Six were weighed out to contain a certain amount of the metal oxide when put into a glass loop. They were shaken together to distribute the metal oxide throughout the Tee-Six. The

mixture was packed into the glass loop by using vacuum and gentle tapping. Glass wool plugs at each end prevented loss of the packing during switching of the Loenco valve and when the loop was activated. The metal oxide was activated by pumping out the loop while it was heated to 130°C, and then by pressurizing with 1 atm O_2. The temperature and the O_2 atmosphere were maintained for 10 hr. The excess O_2 was pumped off, and the loop switched into the helium carrier gas flow. A 10 min blank for CO_2 was run before the experiments began.

The volume of the reactor was measured and the free volume determined by subtracting the volume occupied by the Tee-Six and the metal oxide.

Gas Mixtures

For each run, the pressure of CO was the same 0.680 Torr. This pressure was reached by first measuring a high pressure into a small volume, pressurizing the gas mixing system with 755 Torr He, and mixing thoroughly with the hand operated circulating pump. When oxygen was used, the same procedure was followed except that 157 Torr O_2 was added to the system before the helium was used. Since the total number of slugs reduced the pressure only slightly, a total pressure of 750 Torr was used in subsequent calculations. In some preliminary experiments, water was also added to the gas mixture. Generally, 100% relative humidity was used. This was accomplished by extended recirculation over liquid water in a U-loop section of the system.

BULK REACTOR

Some preliminary experiments were performed using a bulk reactor with MnO_2. A reactor was constructed of quartz and consisted of a chamber 3 cm by 7 cm with an O-ring joint in the center of the reactor. Tubes from each of the longitudinal ends of the chamber are connected to a gas sampling valve (GSV) and a hand operated circulating pump. The total volume of the system was 246 cc, and the pump displaced ~ 80 cc so that the total volume could be circulated in three strokes of the pump. Samples of metal oxide (MnO_2 in this case) on a fritted glass disk were held in the center of the main

chamber by a holder in the O-ring joint. Analysis of samples extracted by the GSV were analyzed gas chromatographically on a Porapak Q column for CO_2.

The reactor was enclosed in a furnace to allow for activation of the MnO_2. Activation was achieved by adding 100 Torr O_2 to a degassed sample of MnO_2 and holding the temperature constant for varying periods of time. In different experiments the temperature was varied from 23° to 110°C.

SECTION V

EXPERIMENTAL PROCEDURES

CFA REACTOR

The helix or cylinder, whichever used, was coated by applying an aqueous suspension of the catalytic material to the supports. The coated supports were placed in the chamber in such a way that the leading edge of the helix or cylinder was about 9 cm from the gas inlet. The chamber was closed and pumped to 10^{-4} for about 4 hr. This ensured complete drying of the sample before experiments took place.

For NO_2 experiments, the conditions were varied between pressures at 700 to 150 Torr with a flow range of 2 to 20 cc/sec. For most of the moisture experiments, 300 mm of argon saturated with H_2O was mixed with 400-mm NO_2-argon mixture. This gave an operational relative humidity at 44%.

NO-O_2 experiments were performed at 190 Torr with an O_2 pressure range between 50 - 150 Torr with the remainder NO-N_2 mixture. The flow was varied between 2 - 20 cc/sec. The photo experiments were performed during the NO-O_2 experiments with lights turned on after the reaction reached a steady state.

CFF REACTOR

A typical experiment began by coating one-half the length of a 20-cm-long 2-cm-dia glass cylinder. One-half of the cylinder was coated because we wanted the gas flow patterns to be established in the cylinder before the gas encountered the catalyst. This procedure eliminated some possible errors in measurements taken near the cylinder edge where gas flow perturbations were taking place. To allow the NO_2 fluorescence to reach the photomultiplier tube, the cylinder was coated such that a narrow strip (6-mm wide) of glass on the cylinder wall was not coated. This window was on the same plane as the laser beam and the optical detection system.

Once the cylinder was coated, it was placed on the movable platform such that the leading edge of the catalyst was displaced 1 cm from the sightline of

the lens-slit system. This was done so that a reference fluorescence intensity could be measured before the NO_2 encountered the catalytic material. The chamber was closed and pumped to 10^{-4} Torr for about 3 hr. Experiments were performed with a 2000 ppm NO_2 in argon gas mixture at a pressure range between 1- and 100-mm and with a flow range of 15 cc/sec to 120 cc/sec. The fluorescence intensity at each point on the cylinder was measured as the point was moved past the lens-slit line of sight. Thus, the fluorescence intensity from the NO_2 should decrease as more catalytic material is moved upstream from the detection sightline. Preliminary experiments were performed with measurements at every 1-mm interval. However, it was found that the necessary information could be obtained by taking fluorescence readings at 5-mm intervals with a 5-sec counting time. It took approximately 1 min to measure the fluorescence intensity over the 45-mm length. The short measuring time was used to reduce the effect of erroneous reading caused by catalytic poisoning.

SLUG REACTOR

For an experimental run with a metal oxide the flow rate was adjusted to 10 cc/min with a needle valve in the helium supply, a GSV loop loaded with the gas mixture (1.81×10^{-8} moles CO/slug), the Loenco valve switched so that the catalyst loop was in the carrier gas, and, then, the GSV switched to send the slug of CO or CO/O_2 through the catalyst bed. Collection was timed for 10 min after the Carle GSV was switched. If more than one slug was used per collection of product, then collection time was started after the last slug, although the $L\text{-}N_2$ was around the collection loop from the first injection. At the end of 10 min, the collection loop was closed off (also the catalyst switched out) and the CO_2 loop heated up to room temperature or above. The carrier flow rate was retimed to 29 cc/min and the CO_2 was "injected" into the carrier gas and analyzed. All experiments were performed at room temperature ($\sim 298^{\circ}K$).

Carbon dioxide calibrations were determined at 29 cc/min, where CO_2 had a retention time of about 1 min (from the CO_2 collection loop) on the Porapak Q column at $50^{\circ}C$. The peak area (half width times height) was

found to be linear with the amount of CO_2 for the range used in the experiments.

BULK REACTOR

For an experiment, 11 Torr CO was admitted to the reactor, the gas volume circulated once (3 pump strokes), and a sample analyzed. Circulation was continued and samples extracted at varying times. Experiments were also performed with 5 Torr of O_2 added with the CO in the same manner. All experiments were performed at room temperature ($\sim$ 298°K).

SECTION VI

RESULTS AND DISCUSSION

RESULTS AND CONCLUSIONS FOR NO_x

General

A number of experiments were carried out in the CFA reactor with solids representative of those materials likely to be found in polluted environments. Data from atmospheric particle loading measurements as well as the catalyst literature were used to aid in the selection of these materials. In addition to low concentrations of NO_x reaction mixtures included O_2, N_2 or A, and H_2O in various combinations. These experiments helped to establish which of the NO_x-solid reactions might be important in polluted atmospheres. Subsequently, more quantitative experiments were conducted using selected NO_x-solid pairs in the CFF reactor.

These experiments led to the conclusion that NO_2 could react with a number of solids likely to be in the environment with rates that could be important in comparison to gas phase reactions. Reaction products included surface nitrates and nitrites as well as gaseous NO.

In the case of NO itself, the experimental results led us to conclude that adsorption or heterogeneous reaction (oxidation or decomposition) does not occur with rates likely to have atmospheric significance.

Moisture was found to have a significant effect on the NO_2-solid reactions. In many cases, materials that were unreactive in "dry" simulated atmospheres were very effective in decomposing NO_2 in humid atmospheres. The results from the "dry" experiments will be discussed first, to be followed by a discussion of the effects of moisture.

Preliminary Experiments (CFA Reactor)

Homogeneous Reactions - When a mixture of NO-O_2-N_2 is passed through the CFA reactor in the absence of any catalytically active solid, NO_2, is formed by a termolecular homogeneous gas phase reaction between NO and O_2. The NO_2 concentration increases with time (distance) as the reaction mixture flows through the chamber. Experimentally (vide ante), the total optical

absorption by NO_2 in the chamber is measured. This can be related to the average NO_2 pressure by using measured absorption coefficients.[16] Results from a typical experiment carried out in the absence of any solids (other than the glass walls of the chamber) are shown in Figure 9. During the first 30 min of the experiment, gas flows were adjusted to the desired values and the system allowed to reach a steady state. From the average NO_2 pressure, and the input gas pressures and flow, we can calculate the rate constant (k_G) for the gas phase reaction by using Equation (20), which is derived in Appendix A.

At t = 50 min, the fluorescent lights were illuminated at half power and the average NO_2 pressure decreased because of its photodecomposition by ultraviolet light passing through the pyrex walls of the reactor. Similar effects were noted when the fluorescent lamps were turned on at full power at t = 63 min. In both illuminated conditions, the steady-state average NO_2 pressures could be used to calculate an effective rate constant for NO_2 production using Equation (20) (e.g., assuming no photodecomposition was occurring). At t = 70 min, the lamps were extinguished and the average NO_2 pressure approached the previous dark steady-state value. At t = 74 min, gas flows were terminated and the system allowed to pump out.

The values for k_G obtained in the absence of any solids are given in the top of Table I. Generally, good agreement was obtained between the values of k_G for the dark reaction and values reported in the literature,[3] although the agreement was slightly dependent on flow conditions. Values of k_G for the dark reaction obtained at low flow (~ 3-cm^3/sec) were in better agreement with the literature values than the rate constants calculated from the high flow experiments. The discrepancy at the higher flow rates is not serious and is considered to be the result of minor mixing or flow problems or both. [In earlier reactor designs, discrepancies of a factor of two or more were not uncommon. Slight modifications of the mixing system and reactor design to avoid areas of retarded gas flow (where more reaction would take place leading to larger effective k_G's) greatly reduced this problem.]

The results from experiments in which the glass helix, coated with selected solid materials, was inserted into the reaction chamber are also

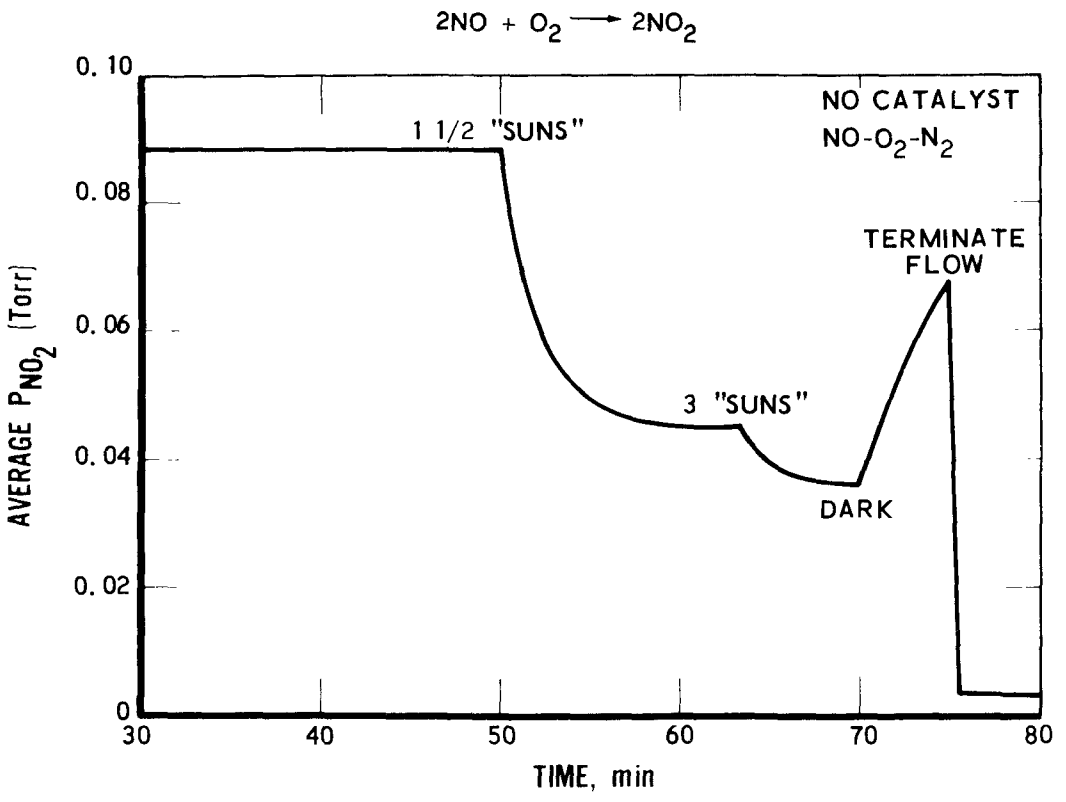

Figure 9. Average NO_2 pressure vs time for an $NO-O_2-N_2$ mixture in the absence of catalysts. The flow rate was 1.4 cm^3/sec and the input pressures of NO, O_2, and N_2 at equilibrium were 0.26, 86, and 102 Torr, respectively.

Table 1. EFFECTIVE VALUES OF k_G FOR THE OXIDATION OF NO IN NO-O_2-N_2 MIXTURES

	Low Flow				High Flow			
	F,	$k_G \times 10^{-3}$, l^2 mole^{-2} sec^{-1}			F,	$k_G \times 10^{-3}$, l^2 mole^{-2} sec^{-1}		
Catalyst	cm^3/sec	Dark[a]	1-1/2 Suns[b]	3 Suns[b]	cm^3/sec	Dark[a]	1-1/2 Suns[b]	3 Suns[b]
None	1.4[c]	7.7	3.0	2.2	8.8[c]	10.9		
	2.8	8.3	4.7		9.8[c]	12.9	9.9	7.9
					12.9[c]	10.0	8.1	6.9
					14.8	9.4	7.7	
None-Average		8.0	3.8	2.2		10.8	8.6	7.4
Charcoal	1.9	~0-5.7[d]		2.6-10.0[e]	9.4	-0-8.0[d]		4.4-9.6[e]
Al_2O_3					9.6	-0-9.7[d]		6.7-13.3[e]
MnO_2[f]					9.7	-0-8.0[d]		8.0-15.5[e]
Fe_2O_3	1.2	6.6	3.5		10.0	8.0	5.8	4.5
Cu_2O	1.8	7.8		3.0	10.0	13.4		6.1
ZnO	2.6	11.2		7.2	9.3	11.0	9.6	7.3
V_2O_5	2.2	9.9		2.9				
	2.2	14.0		3.7				
$(NH_4)_2SO_4$	2.0	8.7		2.9				
$PbCl_2$					9.4	10.6		6.8
Sand					9.6	10.8		6.8

[a] Compare to literature value of $7.5 \pm 0.75 \times 10^3$ l^2 mole^{-2} sec^{-1} (Reference 3)
[b] Approximate equivalent solar intensity with all lamps on at half and full power, respectively
[c] Here only, no helix
[d, e] See text for discussion
[f] Here only, Kapton filter

summarized in Table 1. The materials used were selected on the basis of their known photo- or thermal-catalytic activity for various related reactions (especially oxidation) and/or their likelihood of occurrance in polluted atmospheres (either as airborne particles or ground level exposed surfaces). The various materials used, along with their measured BET surface areas are given in Table 2.

The results for charcoal, Al_2O_3, and MnO_2 were particularly interesting. Initial yields of NO_2 were quite low (actually zero to within experimental error when corrections were made for reaction taking place between the gas inlet and the leading edge of the coated cylinder), compared to the NO_2 produced in the absence of any solid. These results were indicative of surface-catalyzed decomposition of NO_2. (Alternatively, NO could be adsorbed or react at the surface to form products incapable of yielding gas phase NO_2. This possibility was eliminated by the fact that quantitative measurements of NO in the exit gas stream indicated concentrations equal to those in the input gas mixture, except for the small fraction reacting to form NO_2. When O_2 was absent in the reaction mixture, the NO concentrations in the input and exit streams were equal to within experimental error.)

In view of these results, several experiments were conducted with NO_2-N_2 mixtures. A representative example of data from such an experiment with Al_2O_3 is shown in Figure 10. The initial optical density (O.D.) at 480-nm due to absorption by NO_2 for the example illustrated in the figure (as was found in the cases of charcoal and MnO_2) was quite low. To within experimental error, most of this absorption could be accounted for by NO_2 filling the area between the gas inlet (or exit) tube and the leading (or trailing) edge of the coated cylinder. The remaining optical absorption is probably due to the small concentration of NO_2 present along the cylinder axis and absorbing light before it diffuses to the wall where it is removed by adsorption and/or surface reaction.

After several hours, the O.D. begins to rise slowly. This appears to be due to a diminuation or poisoning of the solid reactivity, which permits the NO_2 mixture to penetrate further into the chamber before reaching fresh surface areas where NO_2 can be removed. After many hours ($\sim$ 7 - 8 for the

Table 2. PHYSICAL ADSORPTION SURFACE AREAS

Material	Source	Preparation	Area, M^2/g
Al_2O_3	Activated alumina 214-77	Ground up	196
Al_2O_3	J. T. Baker #0537		233 ± 7
Wood Charcoal Powder	Allied Chemical #1567		40.7
Cement		Ground up	17.9
Fe_2O_3	Commercial jewelers rouge		27.3
PbO	J. T. Baker #2338 yellow powder		20.1
MnO_2	ROC/RIC MN-37		87.5 98.5 ± 2.9[a] 107
Sand	General Chemical	Ground to fine powder	7.3
Fly Ash			15.2
Cu_2O	ROC/RIC CU-33 red 99%		5.5 ± 3.0[a]
ZnO			22.2
V_2O_5	ROC/RIC V-15		14.1
MnO_2	ROC/RIC MN-37 (CO_2/-78 °C)		85.9 119

[a]Errors derived from estimates of error in reading pressure devices, i.e., Matheson 0-760 and voltmeter used with pressure transducer plus a 0.01 V/min drift noted.

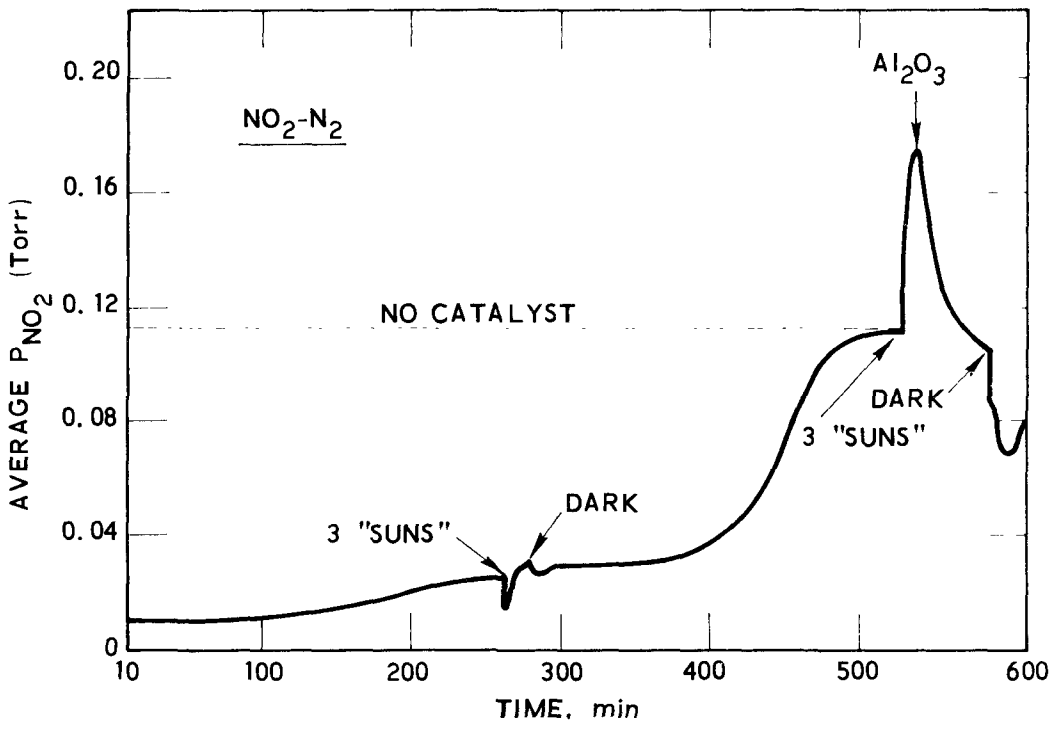

Figure 10. Decomposition of NO_2 over Al_2O_3. Reaction mixture: 0.2% NO_2 in N_2, total pressure was 700 Torr

the experiment in Figure 10), the solid apparently loses all reactivity toward NO_2 and the reaction mixture rapidly fills the area between the end of the helix and the gas outlet. (The magnitude of the final rapid rise in optical density increases as the end of the helix is moved away from the gas outlet and vice versa.) The O.D. obtained at this point in the experiment is approximately equal to that observed in the absence of catalyst, for the same experimental conditions.

The results illustrated in Figure 10 also indicate some interesting photo-effects. Exposure to light (near uv and visible) at ~ 525 min leads initially to a large increase in O.D., probably the result of photodesorption of NO_2 (about 30% of the increase is attributable to scattered light from the fluorescent tubes reaching the photomultiplier). Termination of the light exposure indicates that the O.D. (i.e., NO_2 concentration) has dropped to a level below the value observed at the time the photolysis was initiated. This could be due to photolytic depletion of NO_2 in the gas phase while the lights were on, followed by a gradual return to the "dark" steady-state, and/or photolytic restoration of some catalytic activity. The experiment with MnO_2 (Table 1) suggests the latter explanation as the more probable since the Kapton filter used in that experiment prevents the photolytic dissociation of NO_2 in the gas phase. (Attempts to restore the catalytic activity of Al_2O_3 by subjecting the system to overnight vacuum were unsuccessful.) Exposure to light at ~ 250 min (Figure 10) leads to dramatic effects. Photodesorption is probably occurring here as well; however, the desorbed NO_2 quickly encounters fresh catalyst as it flows downstream, and it again adsorbs or reacts.

Several additional materials listed in Table 1 gave effective values of k_G smaller than (Fe_2O_3) or greater than (ZnO, V_2O_5) those observed in the absence of any added solids when NO-O_2-N_2 mixtures were used. Still others gave effective rate constants equal to those obtained in the absence of added solids. In none of these cases, however, were the effects as dramatic as those obtained for charcoal, Al_2O_3, and MnO_2.

Correlation with the Atmosphere - In order to assess what these data from the CFA reactor experiments mean in terms of potential reactions in urban

atmospheres, we have derived several additional models of our experimental system in Appendix A to include the homogeneous gas phase reaction and a heterogeneous process (either NO_2 decomposition or NO oxidation to NO_2). Using these models, we can then determine the fraction of NO_2-solid (φ_c) or NO-solid (φ_c') collisions leading to reaction. The results of these calculations are given in Table 3.

In a number of cases, values of φ_c or φ_c' lie in the range of 10^{-6}-10^{-8}. These collision efficiencies are orders of magnitude too small to have atmospheric significance.[4] In fact, in no case did φ_c' (the collision efficiency for NO-solid interactions) exceed $\sim 10^{-6}$, and we conclude that the latter reactions are probably unimportant in polluted atmospheres. In the case of NO_2-solid interactions, however, φ_c exceeded 2×10^{-4} for charcoal, Al_2O_3, and MnO_2. Since these approached values required for atmospheric significance, experiments were initiated to examine a broader range of materials for activity in decomposing NO_2.

Extended Studies with NO_2 in the CFA Reactor

Most of these experiments were conducted with NO_2-N_2 or NO_2-A mixtures, and with the glass cylinder rather than the helix for supporting the catalyst. Results from these experiments were analyzed by use of a model for diffusion, flow, and surface reactions in a cylindrical reactor that is described in Reference 23, and Appendix B.

In practice, analytical solutions for the NO_2 concentration as a function of distance along the cylinder axis were obtained by using experimental parameters and various values of φ. These concentration profiles were integrated and compared with the average NO_2 concentration determined from the experimentally measured optical densities.

Results from representative experiments are given in Table 4. The uncorrected NO_2 pressure was calculated from the raw experimental data. A correction was then made for the NO_2 filling the area between the gas inlet and leading edge of the cylinder. The corrected value was compared with those calculated from the model in Reference 23 and Appendix B. Charcoal, Al_2O_3, and MnO_2 gave results consistent with earlier results analyzed with a different

Table 3. FRACTION OF GAS-SOLID COLLISIONS LEADING TO REACTION[a]

	Low Flow				High Flow			
	F,	φ_c (or φ_c') x 10^7			F,	φ_c (or φ_c') x 10^7		
Catalyst	cm^3/sec	Dark	1-1/2 Suns	3 Suns	cm^3/sec	Dark	1-1/2 Suns	3 Suns
Charcoal	1.9	>2000[b]		(0.1)-(1.1)[c]	9.4	>2000[b]		14.4-(0.5)[c]
Al_2O_3					9.6	>2000[b]		2.6-(1.7)[c]
MnO_2					9.7	>2000[b]		(0.1)-(2.1)[c]
Fe_2O_3	1.2	0.5	0.3		10.0	8.0	11.1	14.6
Cu_2O	1.8	0.2		(0.1)	10.0	(0.6)		5.2
ZnO	2.6	(0.4)		(0.7)	9.3	(0.1)	(0.0)	0.3
V_2O_5	2.2 2.2	(0.2) (0.6)		(0.1) (0.2)				
$(NH_4)_2SO_4$	2.0	(0.1)		(0.1)				
$PbCl_2$					9.4	0.0		2.2
Sand					9.6	0.0		3.1

[a] Unbracketed values refer to NO_2 decomposition (φ_c), while values in parentheses are for NO oxidation to NO_2 (φ_c'). Data were taken from the same experiments used to generate Table 1.

[b] These values were calculated from initial optical densities (e.g., t ≈ 10-100 min in Figure 9). They essentially represent a lower limit for φ_c, due to experimental sensitivity limits. Near the end of these experiments (e.g., t ≈ 500 min in Figure 9), calculated values of ~ 2-8 x 10^{-7} were obtained for φ_c.

[c] As determined from the peak and steady-state O.D.s at the end of the experiment (e.g., t ≈ 540 min and t ≈ 85 min, respectively in Figure 9).

Table 4. INITIAL OPTICAL DENSITIES IN NO_2 - N_2 EXPERIMENTS

CATALYST	P_t (Torr)	F (cm^3/sec)	NO_2 (%)	AVERAGE P_{NO_2} (Torr)		
				UNCORRECTED	CORRECTED	CALCULATED*
Al_2O_3	688	13.5	0.2	0.448	0.180	0.176
	312	10.3	0 2	0.152	0.030	0.031
	204	13.3	0.2	0.104	0.024	0 018
	688	5.2	0.2	0.309	0.037	0 075
	689	12.0	0.05	0.097	0.029	0 039
Al_2O_3	691	12.3	0.05	0.096	0 028	0.040
CHARCOAL	688	14.3	0 2	0.472	0.204	0 184
MnO_2	687	14.0	0.2	0.484	0.212	0.180
PbO	688	12.8	0.2	0.496	0.228	0.164
CEMENT	691	12.2	0 2	0.432	0.168	0 160

*Assuming $\phi \geq 1 \times 10^{-4}$

model, namely, $\varphi > 10^{-4}$. Lead oxide and cement were also found to be reactive. However, other materials, including fly ash, soil, and crushed oleander leaves, were unreactive ($\varphi < 10^{-7}$).

A number of experiments were conducted to identify products of the heterogeneous NO_2 decomposition reaction. The results from one such experiment are plotted in Figure 11. In that experiment, the average NO_2 pressure and NO concentration were measured as a function of time. The average NO_2 pressure increased as before. Gaseous NO was also detected in the effluent gas, but only after a substantial induction period. The results illustrated in Figure 11 are representative for most of the reactive materials. In general, the NO concentration in the effluent was $\sim$ 40 - 60% of the NO_2 in the influent reaction mixture. (The NO_2 was completely destroyed during transit through the reactor except at the end of the experiment, where the solid became totally unreactive.) As discussed earlier, in separate experiments with NO-N_2 or NO-A mixtures, NO did not adsorb or react on these surfaces.

Additional experiments were conducted to determine the composition of nitrogen compounds deposited on the solid surfaces. Wet chemical methods were used for NO_2^- and NO_3^- determinations.[24] In general, these experiments were run only for a short period of time to avoid poisoning of the solid surface. In some cases, after the experiment, the solid was removed in segments, washed, and the washings analyzed for NO_x^-. Results from one such experiment with NO_2-N_2 over Al_2O_3 are illustrated in Figure 12. The prominent surface species after reaction was NO_2^-, with a small amount of NO_3^-, although, for convenience, we have plotted the total $NO_2^- + NO_3^-$ as NO_3^- in Figure 12. The points in the figure were calculated using the model in Reference 23 and Appendix B, and were normalized for absolute comparison with the experimental data using the total NO_2 flux into the reactor during the experiment. For the most part, the calculated and experimental results are in good agreement. The biggest discrepancy is at $Z < \sim$ 1-cm, where expected edge effects would give discrepancies in the directions observed. Quantification of the latter effects would be difficult in this system, although they could be reduced or eliminated by leaving the first few cm of the cylinder uncoated. Additional qualitative

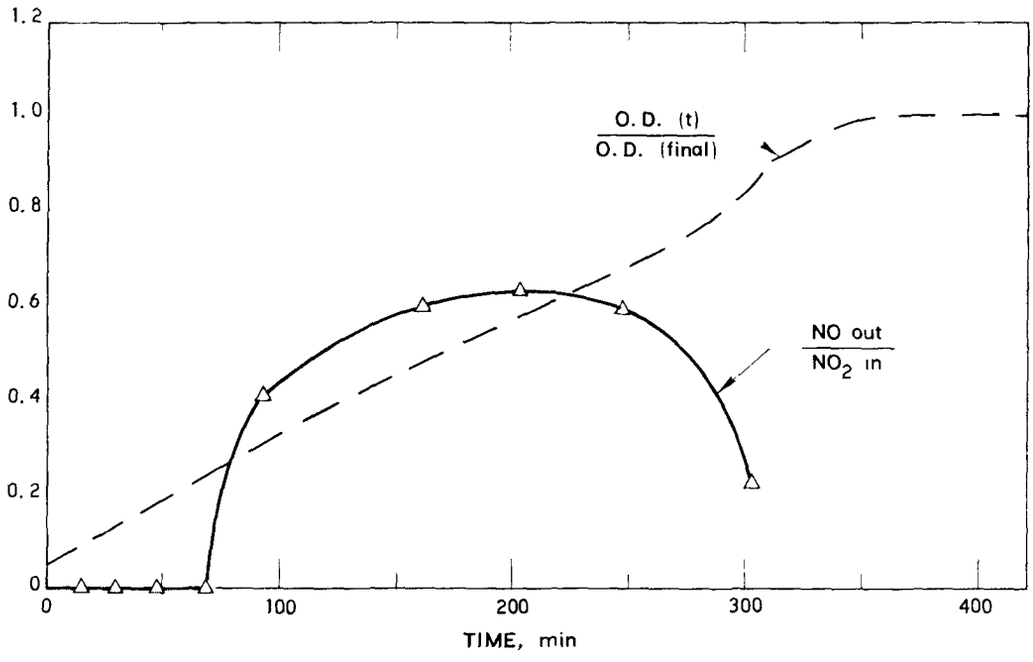

Figure 11. Decomposition of NO_2 over MnO_2. Reaction mixture: 0.2% NO_2 in N_2, total pressure was 700 Torr

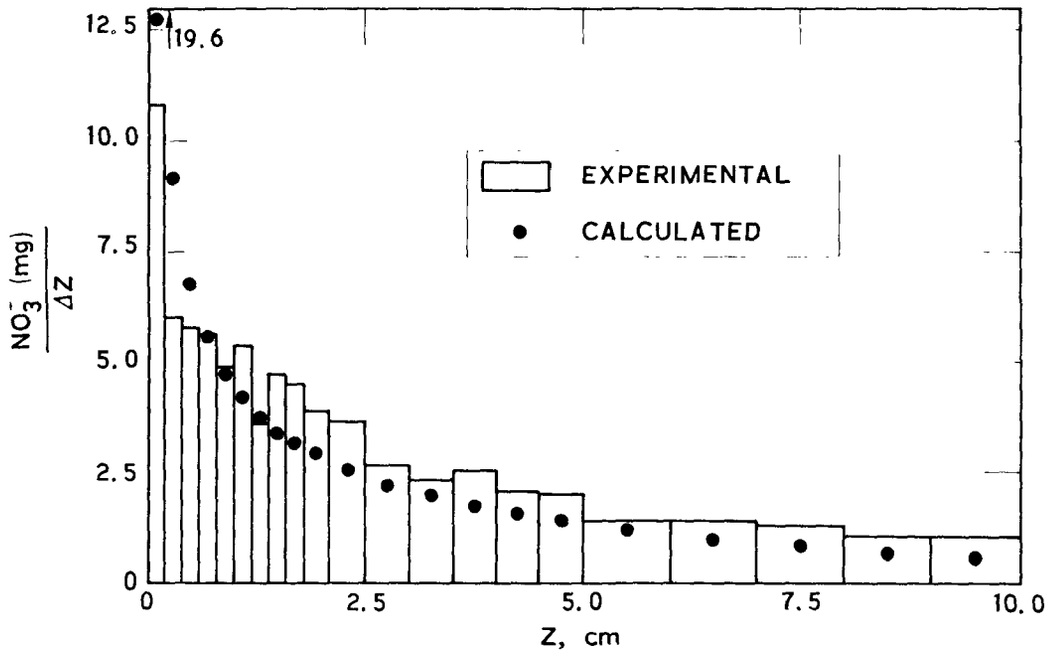

Figure 12. Surface nitrogen compounds (as NO_3^-) from the decomposition of NO_2 over Al_2O_3. Reaction mixture: 0.2% NO_2 in N_2, total pressure was 700 Torr

and quantitative results are given in Table 5.

Several comments should be made regarding the NO_x^- results. First of all, gaseous NO_2 bubbled through water gave a positive test for NO_2^-, suggesting that both adsorbed NO_2 and NO_2^- would give positive tests for NO_2^-. In addition, the mere act of "washing" the solids might result in chemical reaction. For example, adsorbed NO_2 might dissolve in water and react with surface OH groups to form NO_3^-. Thus, the NO_x^- results should be considered cautiously. The latter comments especially also apply to results obtained when water was added to the reaction mixture and greatly enhanced reactivities were observed (see below).

CFF Reactor Experiments

Gaseous mixtures in the CFF reactor were generally limited to NO_2 plus N_2 or A. The NO_2 concentration (detected by laser excited fluorescence) was measured as a function of distance down the cylinder axis. Results from a typical experiment are illustrated in Figure 13. The solid curve in the figure was calculated using the model for diffusion, flow, and wall reactions described in Reference 23 and Appendix B. The latter solution is a Bessel series that reduces to a single exponential term at large distances. An example of the exponential decay with distance at large distances is illustrated for data from another experiment in Figure 14.

Data from experiments conducted in the CFF were analyzed by comparing measured NO_2 concentration profiles to those obtained from the analytical model for various values of φ. Results from experiments with charcoal conducted in cylinders with radii of 0.50- and 0.95-cm are given in Table 6 for various experimental conditions. The average φ of 1.6×10^{-3} would give a particle limited lifetime for NO_2 in polluted atmospheres of $\sim$ 1 hr, using the model in Reference 1. Results for MnO_2 exhibited somewhat more variation with $\varphi \approx 0.3 - 3 \times 10^{-3}$, whereas, Al_2O_3 gave $\varphi \approx 3 \times 10^{-4}$.

Effects of Moisture - Moisture greatly extended the reactivity of those materials discussed above that were found to decompose NO_2. Alternatively, the activity of a solid destroyed via the "dry" reaction, could be restored and significantly extended by adding water to the reaction mixture. Examples of the latter

Table 5. ANALYSIS OF NITROGEN COMPOUNDS ON CATALYST SURFACE

	SURFACE NITROGEN COMPOUNDS		TOTAL (mg) AS NO_2	
CATALYST	NO_3	NO_2	EXPT	CALCULATED
Al_2O_3[a]	SMALL	LARGE	24 19 0.8	24 14 1.0
Al_2O_3[b]	LARGE	SMALL	-	-
CHARCOAL	LARGE	SMALL	-	-
MnO_2	LARGE	SMALL	-	-
PbO	SMALL	LARGE	-	-

[a]Analabs chromatographic grade activated alumina

[b]J. T. Baker "Reagent" Al_2O_3

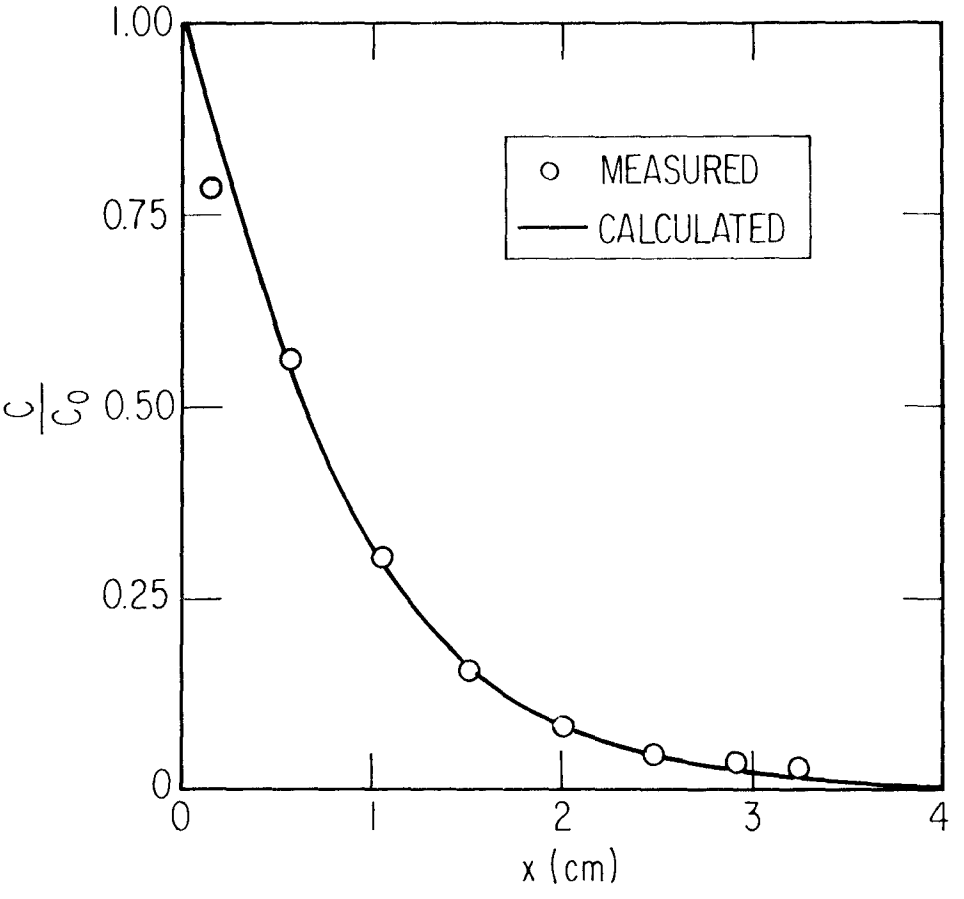

Figure 13. Decomposition of NO_2 over charcoal. Relative concentrations of NO_2 (equal to relative fluorescence intensities) vs distance for a 0.2% NO_2 in a mixture at 10 Torr

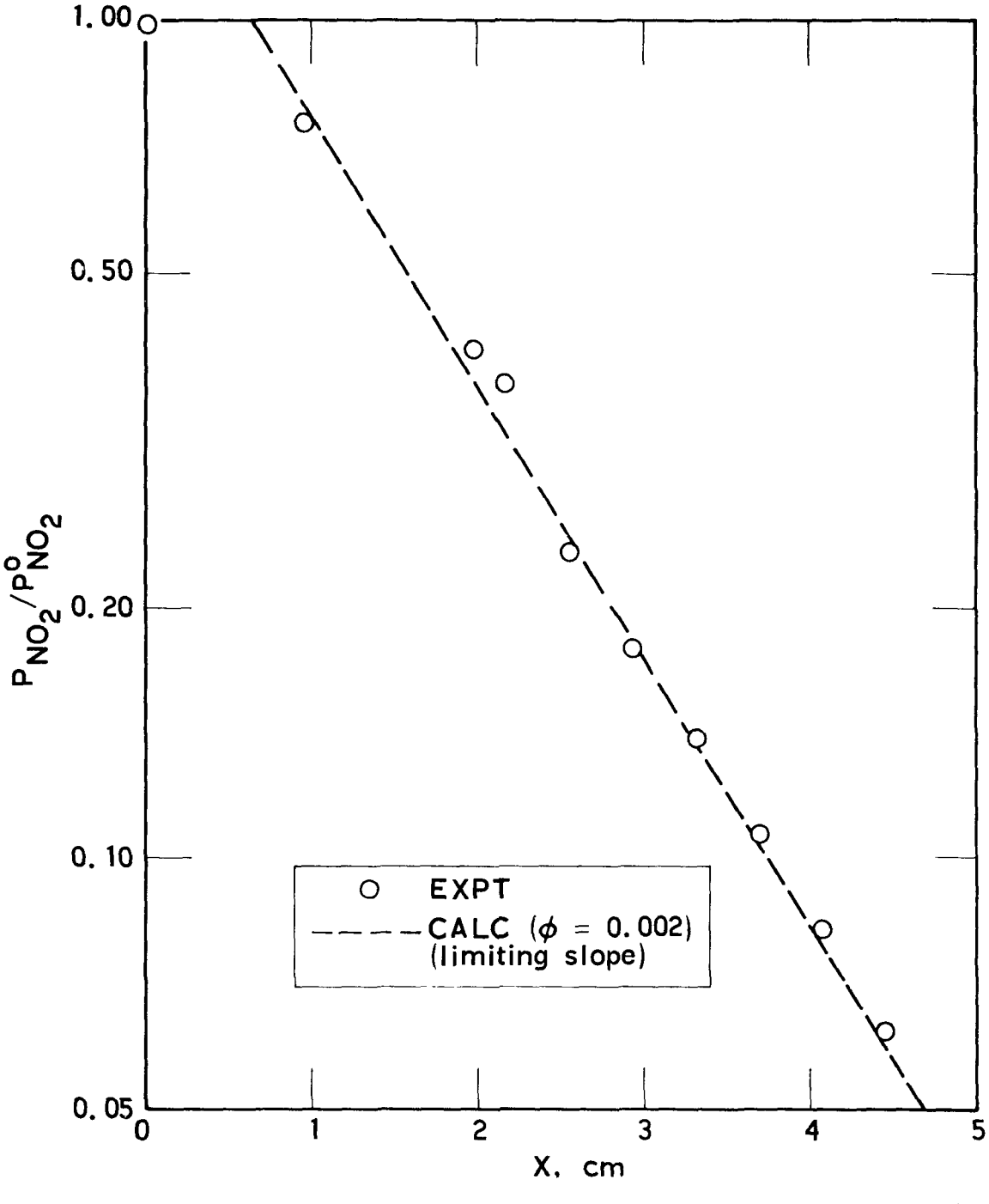

Figure 14. Decomposition of NO_2 over MnO_2. Relative pressures of NO_2 (equal to relative fluorescence intensities) vs distance for a mixture at 10 Torr

Table 6. RESULTS FOR NO_2 - A MIXTURES OVER CHARCOAL

r, cm	P, Torr	F, cc/sec	$10^3 \cdot \varphi$
0.50	1.0	17.5	2.6
	9.9	25.0	1.2
	10.2	16.5	1.4
0.95	1.0	0.4	1.5
	1.0	0.4	1.0
	9.8	1.7	1.6
	10.3	1.7	1.6

φ (average) = 1.6×10^{-3}

τ (atmosphere) $\approx$ 66 min

experiments are shown in Figure 15. An NO_2-A mixture was passed through the cylinder that was coated with a minimal amount of solid in a band $\sim$ 1 in wide. After $\sim$ 20 - 60 min, depending on the solid, the reactivity toward NO_2 was destroyed. Subsequent addition of moisture restored and greatly extended the activity observed under dry conditions.

More important, experiments in the CFA reactor indicated that virtually all of the materials listed in Tables 1 and 2, even those that were unreactive under dry conditions, effectively decomposed NO_2 ($\varphi > 10^{-4}$) when moisture was present (43 - 44% RH). Of the materials listed, $PbCl_2$ was not tested; $(NH_4)_2SO_4$ exhibited minimal activity ($\varphi < \sim 10^{-5}$). We also examined CaO and particulate matter collected from the environment on glass fiber filter paper. Both materials gave $\varphi > 10^{-4}$; however, the results for the particulate matter from the environment are equivocal since the filter paper itself was found to decompose NO_2. The latter result could have important implications in particle collection measurements if surface NO_x^- is formed.[25]

Summary of NO_x Reactions on Solid Surfaces

The results for NO_2 suggest that this pollutant could be heterogeneously destroyed in the atmosphere with a lifetime of $\sim$ 1 hr, if actual airborne particles had reactivities similar to those of charcoal and MnO_2 in our laboratory experiments. This reaction is greatly facilitated by moisture in the presence of many solids likely to be found in polluted environments. Quantitatively, the reaction transforms NO_2 to NO and $NO_{x\,(ads)}^-$, and leads to a substantial reduction of NO_x in the gas phase.

The 1 hr lifetime suggests that particles could be an important nighttime sink for NO_x. In addition, although this rate is slow compared with the noontime photolytic lifetime of NO_2 in the atmosphere (2 - 3 min), the heterogeneous process leads to a net reduction in oxidant concentration ($NO_2 + O_3$). The photolytic process does not. Thus, the overall effect of the heterogeneous process could be more important than the light-initiated decomposition.

We have considered only airborne particulate matter ($\sim 100 \mu g/m^3$) in our modeling. Consideration of ground level surfaces could greatly enhance total reactivity. Moreover, reactions taking place on the latter surfaces could

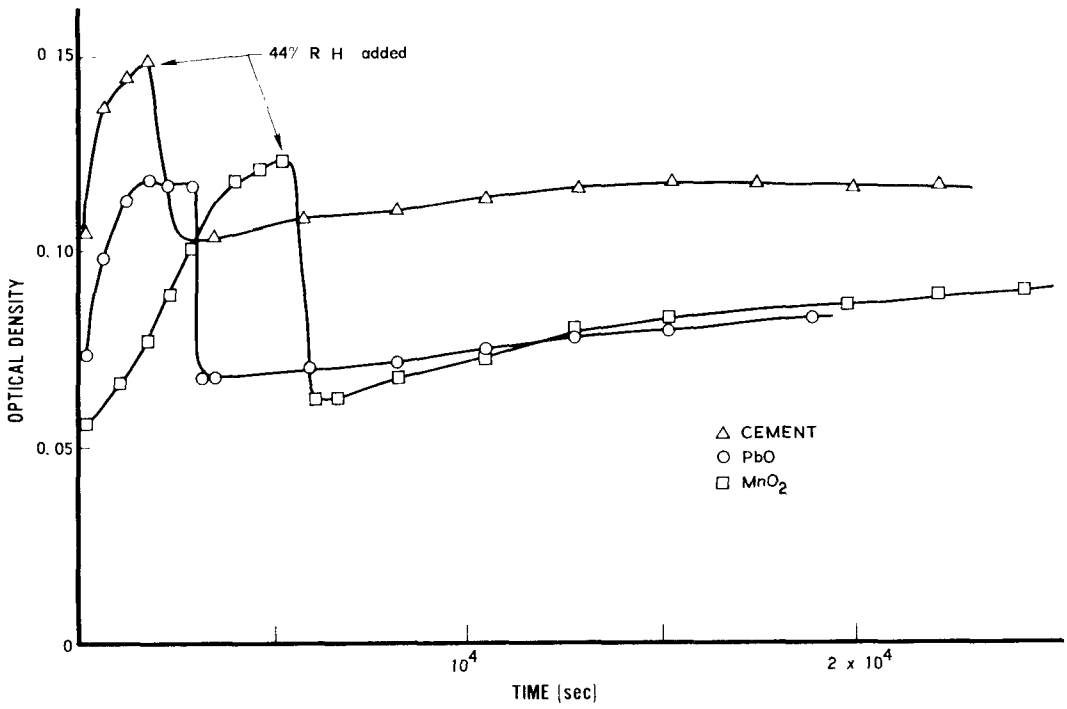

Figure 15. Effects of moisture on NO_2 decomposition

lead to concentration gradients near the ground, depending on the amount of transport mixing taking place. These gradients could be significant in accurately assessing pollution related health problems.

Finally, NO exhibits only minimal activity toward solids examined in this study. Based on quantitative rate measurements, we conclude heterogeneous atmospheric processes of NO are probably unimportant.

RESULTS AND CONCLUSIONS FOR O_3

Several exploratory experiments were conducted with O_3 and various solids. Gas mixtures containing ozone prepared for chemiluminescent detection of NO (Figure 3) were instead fed into the CFA reactor. The average O_3 pressure in the reactor was determined by measuring optical absorption at 313-nm and experimental absorption coefficients.[26] Here, as in the case of NO_2, we found that $\varphi > 10^{-4}$ for charcoal and MnO_2, whereas $(NH_4)_2SO_4$ was unreactive. In the case of Al_2O_3, $\varphi < 10^{-5}$ was determined. Except for $(NH_4)_2SO_4$, the effects of moisture were not examined. Water did appear to lead to some decomposition of O_3 in the presence of $(NH_4)_2SO_4$. However, reactivities were low and of the order of experimental uncertainties.

For O_3, as in the case of NO_2, we conclude that the heterogeneous reaction of ozone in polluted atmospheres could be important and lead to an overall reduction of the total oxidant concentration.

RESULTS AND CONCLUSIONS FOR CO

The results of the study may be divided into two parts: (1) the bulk reactor and development of the slug reactor; (2) the slug reactor. In the first part, some valuable observations and kinetic analyses were obtained, but the initial rates of reaction were not determined. These will be discussed first, then the slug reactor results will follow. In all preliminary studies, MnO_2 was the only metal oxide used since it is known to oxidize CO to CO_2 at ambient temperatures.[10] Subsequent to the early treatment of the data, Kobayashi and Kobayashi[10, 11, 12] showed that MnO_2 is quite reactive even at lower temperatures.

Bulk Reactor

Results from the bulk reactor do not yield initial rates since the large volume of the reactor and the time required for circulation integrates the product CO_2 over fairly large time intervals. Also, problems arising from the failure to regenerate the MnO_2 to the same activity level resulted in extreme data reduction problems in the depletive oxidation studies (without oxygen present). The data with oxygen were even more intractable. Corrections were made for the varying initial metal oxide reactivity, and the data were reduced as described below.

To treat the data, the form of the rate equations must first be considered. Equations (2) and (3) yield a rate expression for CO loss.

$$-d(CO)/dt = k_b(A)^n(CO)^m + k_c(B)^p(CO)^r + \ldots \quad (6)$$

where A and B are the concentration or number of active sites of each type. The data from the bulk reactor experiments were reduced by assuming a first order dependence in CO ($m = r = 1$) and plotting the log of the interval average rate $[\ln(\Delta p_{CO_2}/\Delta t \times p_{CO})]$ vs time. This allows each experiment to be normalized to the same MnO_2 activity by adjustment along the time axis. Figure 16 shows the raw data for two separate depletive oxidation runs that emphasize the difference in metal oxide activity. Figures 17 and 18 show the results of the data reduction procedure for all experiments for the depletive studies and studies with added oxygen respectively. Figure 17 shows that, although the scatter is great, a general trend is obvious, and a line can be drawn to fit the data. These data best fit the rate law,

$$-d(CO)/dt = k_1(CO)\, A_o\, e^{-k_1 t} + k_2(CO)\, B_o\, e^{-k_2 t}. \quad (7)$$

It does not fit a single first or second order dependence in active sites. A_o and B_o are the initial activity of the metal oxide samples (number or moles of active sites). Two tangent lines can be drawn in Figure 17 associated with the two parts of (7) each having the form

$$\ln(\Delta p_{CO_2}/\Delta t \times p_{CO}) = k_1 t - \ln k_1(CO)A_o \quad (8)$$

From this equation, the initial rate constant for oxidation k_1 and the number

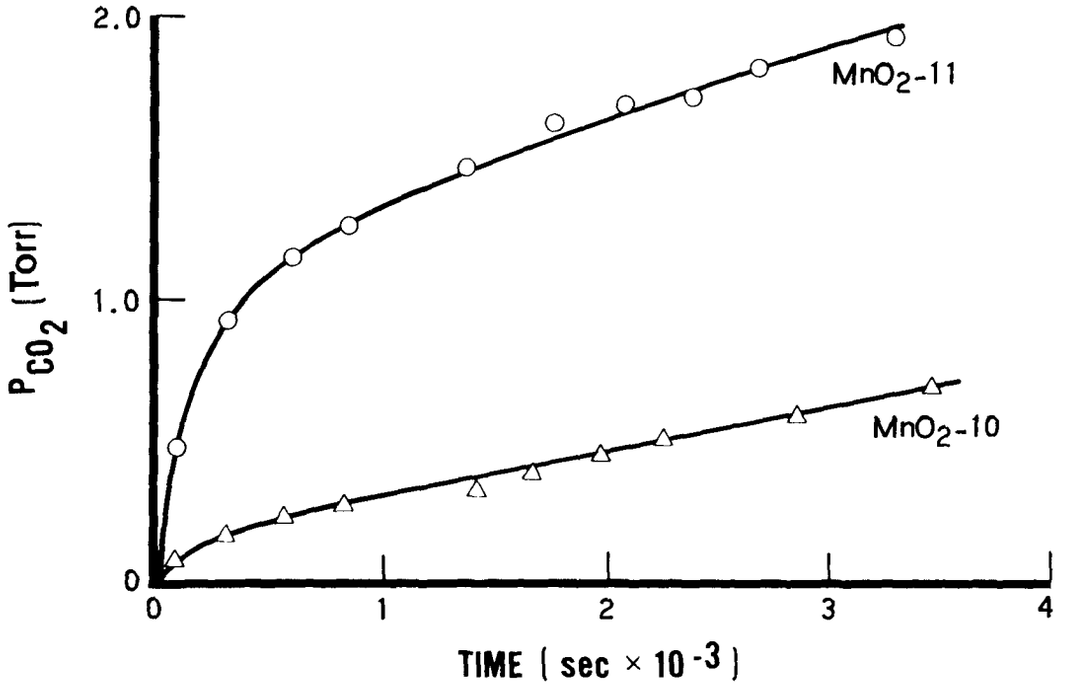

Figure 16. Pressure of CO_2 vs time. 11 Torr CO, 200 mg MnO_2.

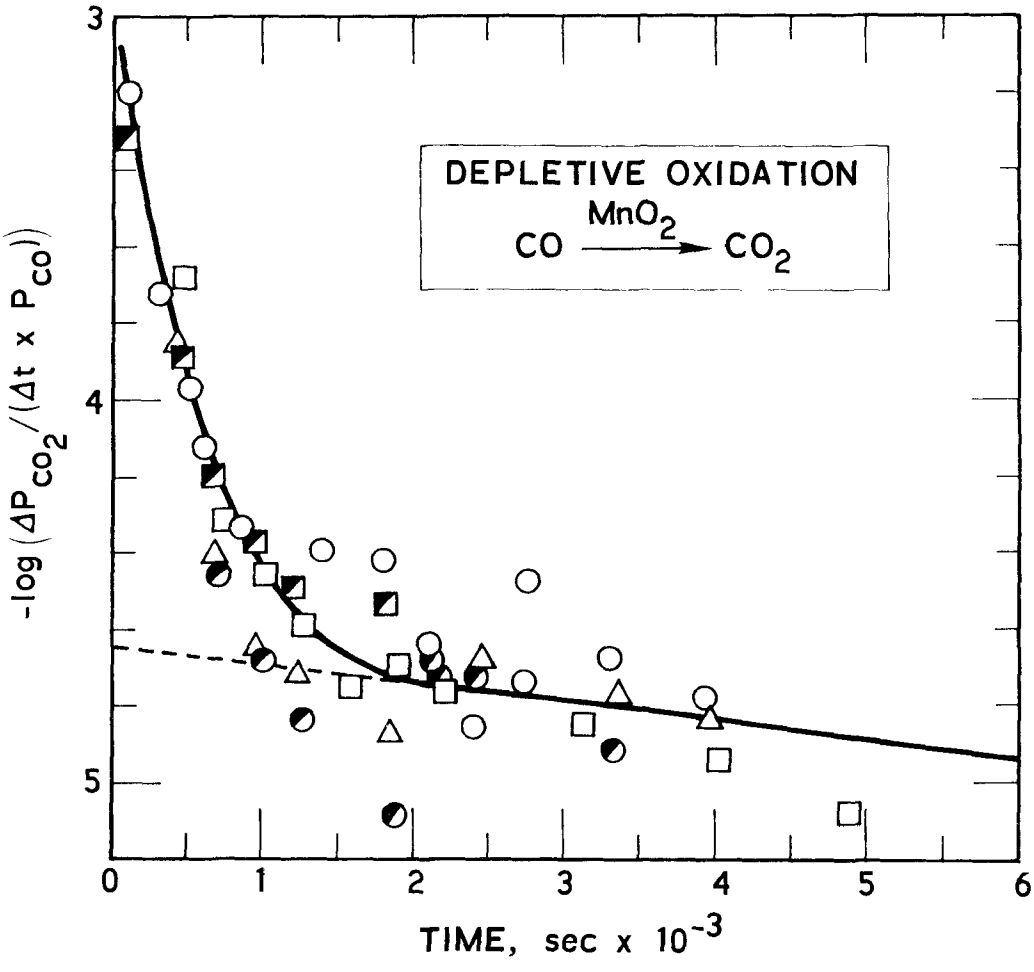

Figure 17. Depletive oxidation of CO

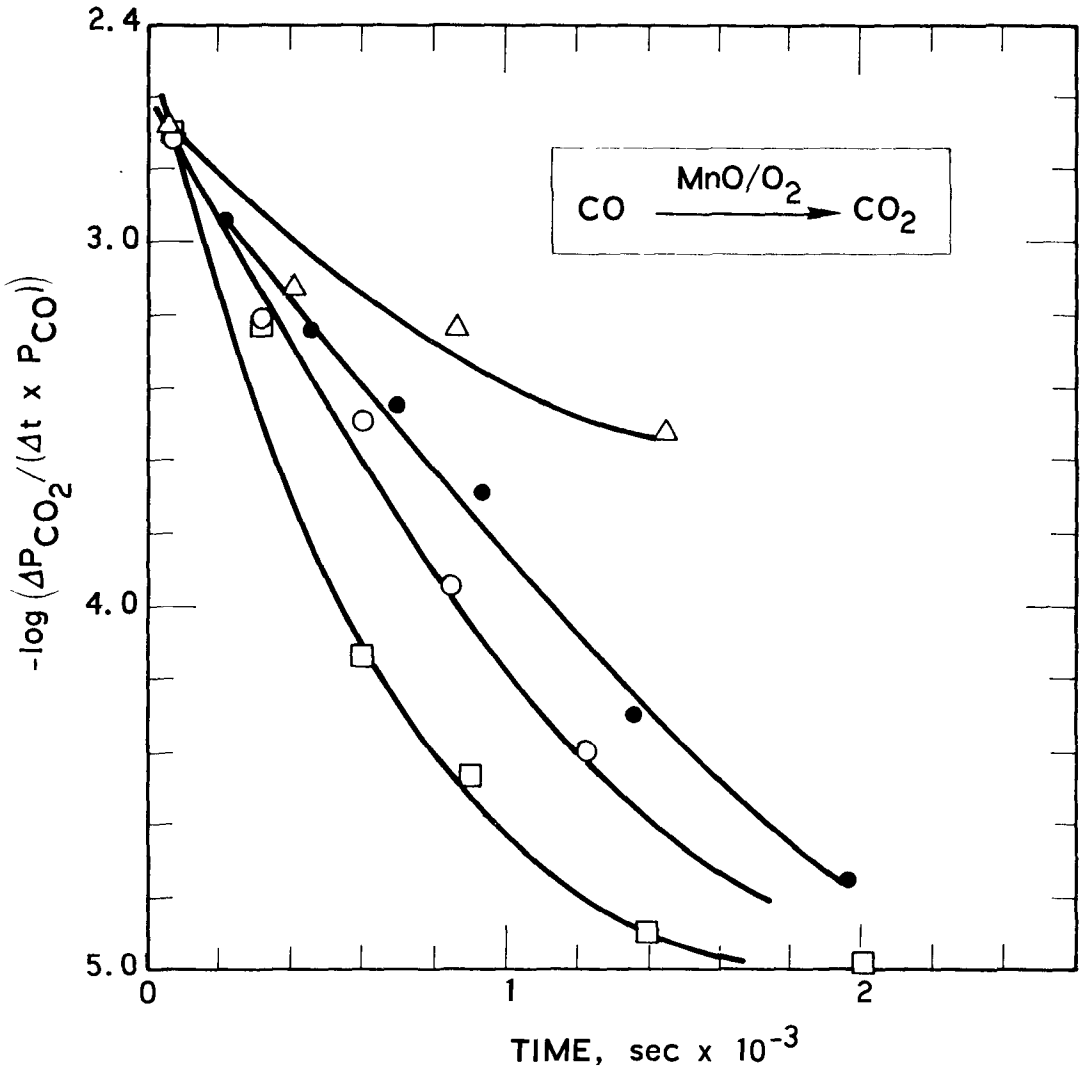

Figure 18. Oxidation of CO in the presence of O_2

(or concentration) of active sites may be derived. It was found that $k_1 = 351$ moles^{-1}sec^{-1} and $A_o = 9.5 \times 10^{-5}$ moles/g. The rate constant is a minimum due to the integration of the raw data; however, extrapolating this value to the atmosphere with a MnO_2 loading of $10\mu g/m^3$ and the measured activity yields a CO lifetime of 0.1 yr.

The data with oxygen present are more complex because of the regeneration of sites by reactions (4) and (5). The inaccuracies of the data preclude a similar analysis. It was observed, however, that addition of even 5 Torr of O_2 did increase the initial rates by factors of three or so. If a mechanism similar to that proposed (reactions 2 - 5) is operating, the observation indicates that the initial rate constant for oxidation is even higher. Kobayashi and Kobayashi performed a series of experiments using the transient response method on the MnO_2 + CO (+ O_2) system at -26° and proposed a mechanism that agrees quite well with ours.[10, 11, 12]

Slug Reactor

Preliminary Experiments - The originally constructed slug reactor did not have the sensitivity to allow improvement in the results from the bulk reactor. Several experiments were performed to establish the parameters necessary for later experiments (such as flow rates and metal oxide loadings). Although quantitative data were not recovered, several observations were important. It was found that the rate of loss of CO from the slug was unaffected by large pressures of CO_2. This confirmed the earlier conclusion from the kinetic analysis of the bulk reactor results that CO_2 does not affect the activity or the capacity of MnO_2. Experiments were also performed in which the slugs were saturated with water vapor. Again, no change in the activity or capacity could be detected.

Detailed Experiments - Several different processes involving metal oxides could result in oxidation of CO in the atmosphere. Overall any process must be catalytic since the metal oxide loadings in the atmosphere are generally low. Using the generalized equations this means that,

$$k_2(CO) \text{ or } k_3(CO) \gtrsim k_4(O_2) \text{ or } k_5(O_2) \qquad (9)$$

At least three types of catalytic behavior could be included in this requirement: 1) oxidation of CO by a stable active site, A, followed by regeneration of the site by O_2; 2) oxidation of CO by a labile, active site followed by regeneration; 3) the activation of O_2 by the site which would then oxidize CO. The purpose of the detailed experiments was to determine if any of these processes were possible contributors to the atmospheric CO sink. The study was done in two parts: depletive oxidation where the metal oxide was activated and then depleted by CO; and oxidation with oxygen present.

In a slug-type reactor, the solid reactant is placed in a section of a flowing non-reactive gas stream. The other reactants are introduced in slugs or pulses by some dosing device (here a gas-sampling valve) and plug flow is assumed. The slug of reactant then reacts as it passes through the solid reactant section and is analyzed on exit from the reactor. The data available are the initial and final reactant product concentrations in the slug, the flow rate (which is related to the residence time and free volume over the reactant), and the slug volume. Assuming that we have only one type of site with a rate of oxidation that is large enough to be detected, the rate of CO loss is,

$$-d(CO)/dt = k_r A(CO). \qquad (10)$$

A is the effective concentration of active sites and is directly related to the metal oxide activity. k_r is actually the product of the rate constant (k_2) times the equilibrium constant K_{11},

$$CO_{(g)} \rightleftharpoons CO_{(ads)}. \qquad (11)$$

This equilibrium was found to be rapid under our conditions since no broadening of the CO slug was observed and the combination of the rate constant and the equilibrium constant is justified.

In these slug type experiments each slug is considered separately and is in fact a separate experiment. Under depletive oxidation conditions where

the activity of the metal oxide bed, that is, the effective concentration of A, does not change appreciably during the passage of single pulse through the bed, equation(10)may be integrated with respect to CO. $(CO)_o$ and $(CO)_i$ are outflow and inflow

$$-\ln\left[(CO)_o/(CO)_i\right]_n = k_r A_n \Delta t \qquad (12)$$

concentrations respectively, A_n is the effective active site concentration for the n^{th} slug, and Δt is the slug transit time. Equation (12) may be written,

$$-\left[\ln(CO_o)/(CO)_{i_n}\right]/\Delta t = k_r' A_o - k_r (CO_2)_T, \qquad (13)$$

where A_o is the initial concentration of active sites, and k_r' is the effective rate constant under the assumptions. $(CO_2)_T$ is the total CO_2 produced through slug number n. The form of 12 will yield a linear relationship between the left-hand side and $(CO_2)_T$ when either $(CO)_i - (CO)_o \ll CO_i$ or $\Delta A \ll A_o$, however, when neither of these conditions are met,curvature will result. All experiments were performed under one or the other of the proper conditions. 12 is useful for two reasons, first it provides a convenient method of data presentation, and second, it allows one to determine A_o. The data for both depletive oxidation and the oxidation with O_2 present and the linear relationships are shown in Figures 19-22. The experimental conditions are shown in Table 7.

The complete equation that must be used to determine the rate constants is,

$$d(CO_2)/dt = k_r\left[A - (CO_2)\right]\left[(CO) - (CO_2)\right]. \qquad (14)$$

This equation treats the instantaneous concentrations of reactants and the gradients that develop during the passage of the slug through the reactor bed. The integrated form of 13 was used to determine k_r for each slug. The approach was to divide the metal oxide bed into ℓ arbitrary sections of equal length and the CO pulse into $\mathcal{M}$ sections of the same length. Square pulses

Table 7. CONDITIONS USED IN METAL OXIDE OXIDATIONS: SLUG MICRO-REACTOR

Metal Oxide	Wt. Metal Oxide, g	Concentrations in Each Slug (at 1 atm)[a]	
		CO, $\times 10^8$	O_2, $\times 10^6$
MnO_2	0.0117	3.63	0
	0.0117	3.63	8.28
CuO	0.157	3.63	0
	0.157	3.63	8.28
ZnO	0.0915	3.63	0
	0.0915	3.63	8.28
Fe_2O_3	0.296	3.63	0
	0.296	3.63	8.28

[a] $O_2/CO = 228$

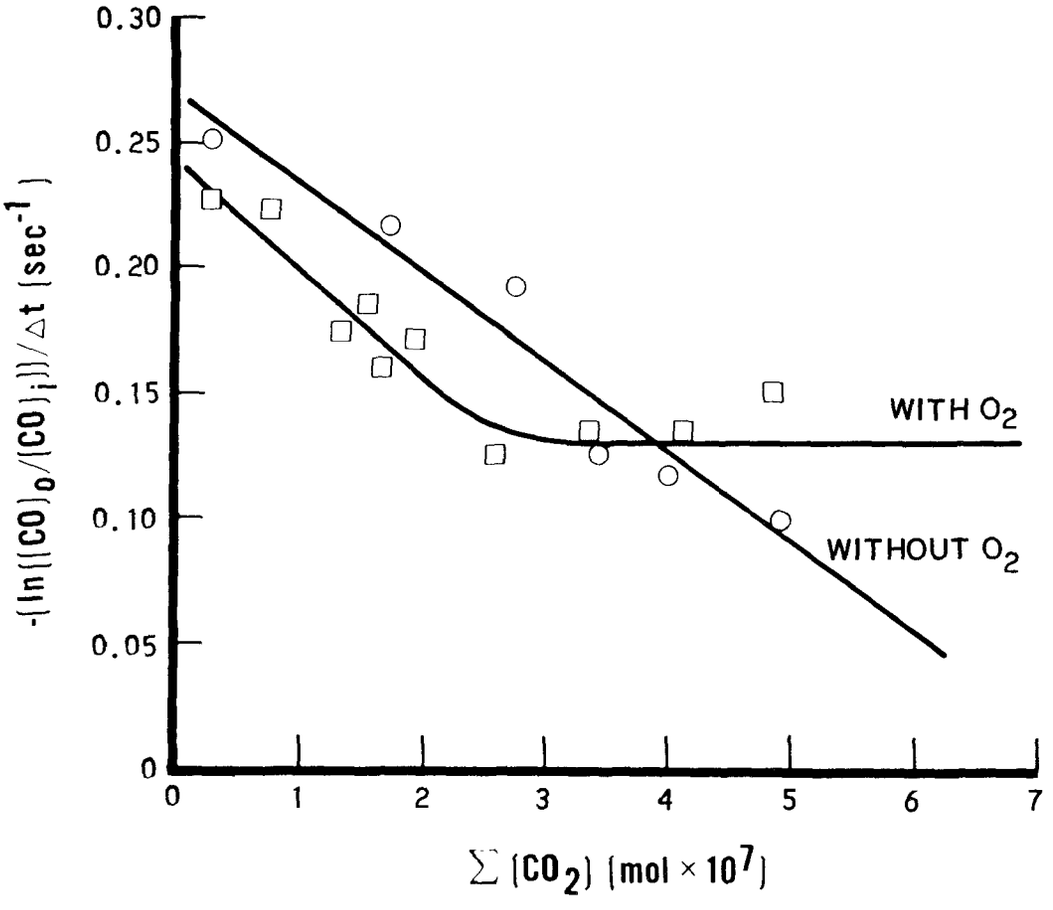

Figure 19. Slug reactor data: manganese dioxide

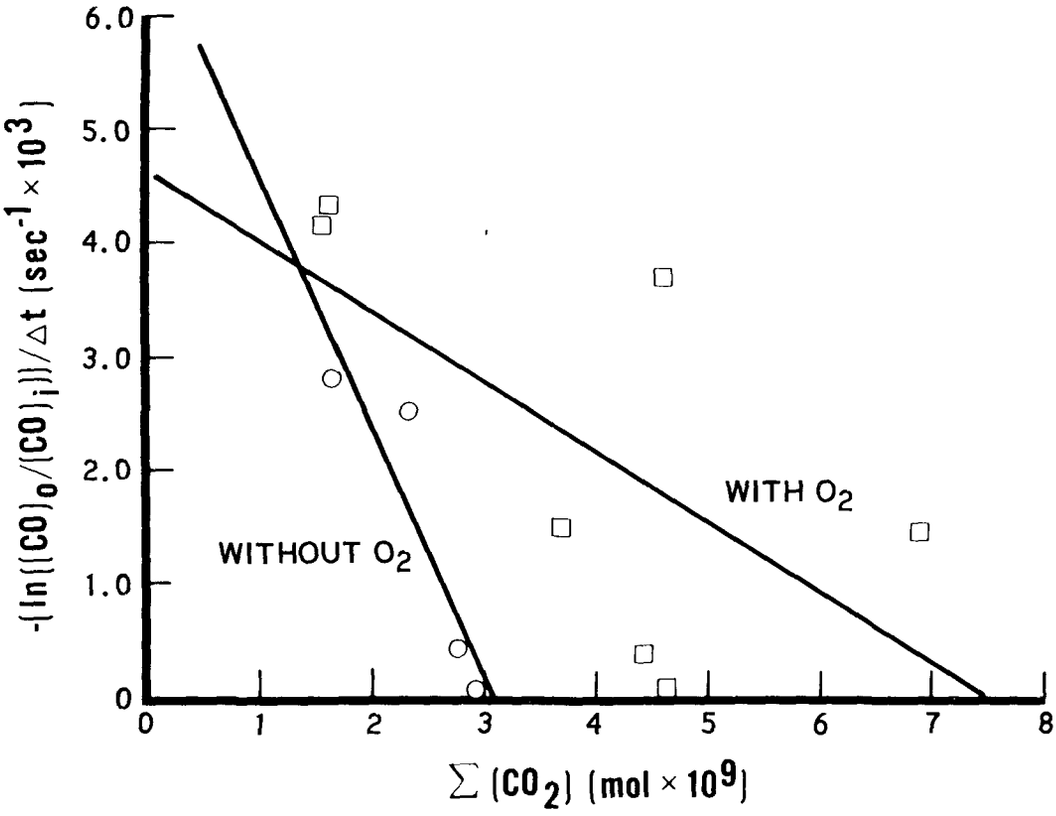

Figure 20. Slug reactor data: zinc oxide

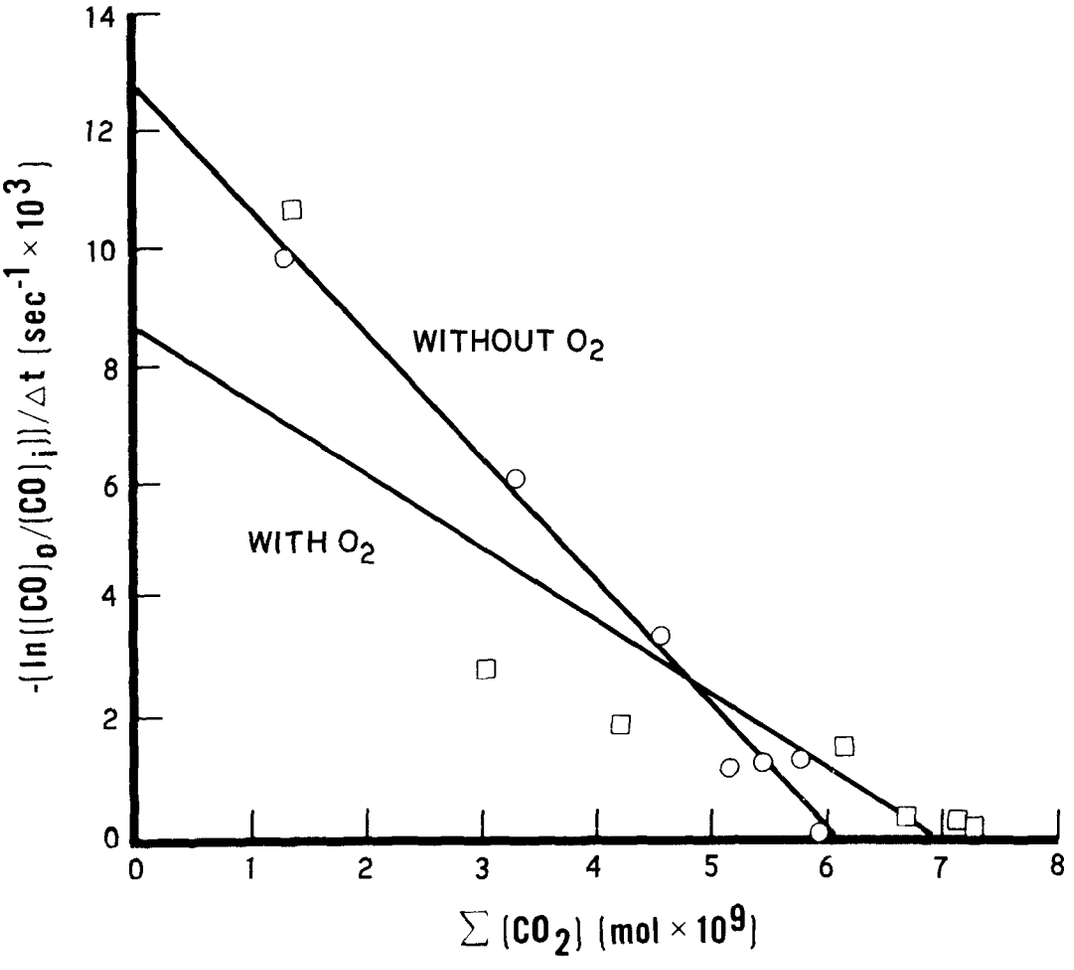

Figure 21. Slug reactor data: cupric oxide

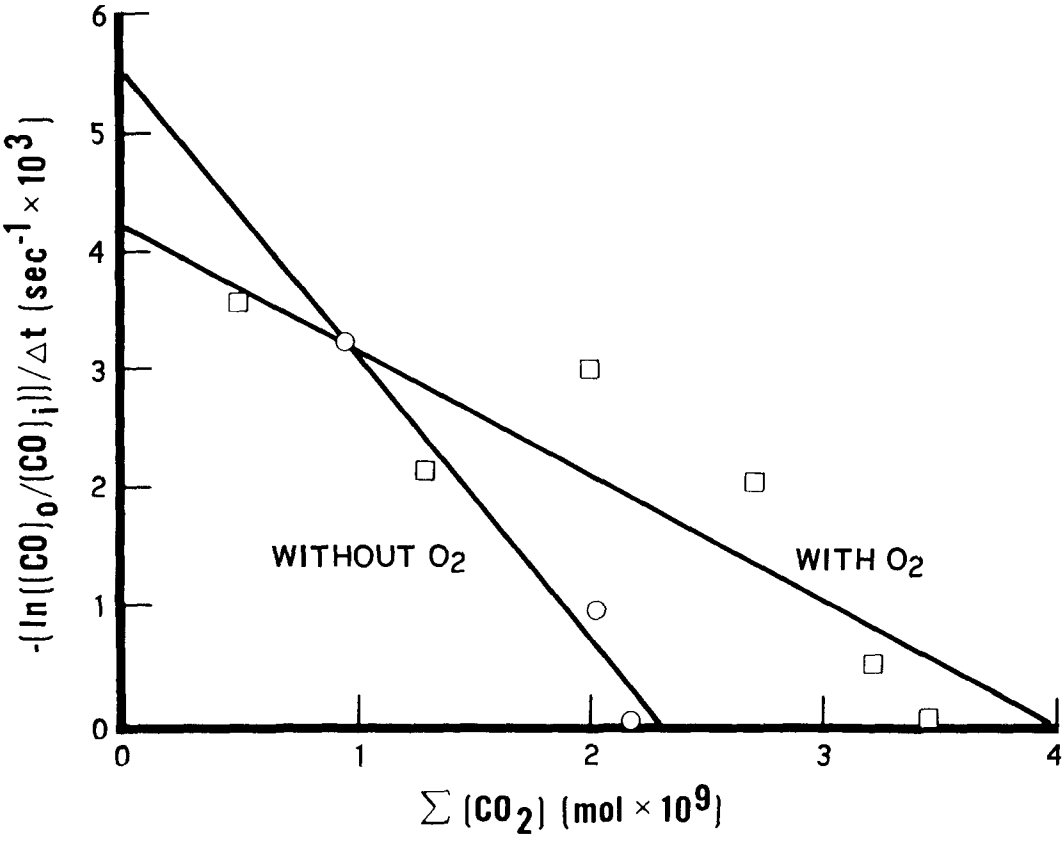

Figure 22. Slug reactor data: ferric oxide

and homogeneous M_xO_y distributions were assumed. The integrated form of 13 was then solved for each ℓ and, $/\!/$ and the resultant concentrations of CO_2, CO, and A used for each subsequent calculation. The $(\ell \times /\!/)$ moles of CO_2 produced in each slug was then compared with the experimental value and the value of k_r found by iteration to converge the two values. Each slug should yield an identical value of k_r if the mechanism is correct and if A_o has been determined correctly.

The results of the analysis of the depletive oxidation of CO by metal oxides are shown in Table 8. Using the initial activity, A_o, the maximum rate constant for oxidation in the atmosphere, k_rA_o, may be used to estimate the possible effect of metal oxide oxidation on the lifetime in CO of the atmosphere. This condition would correspond to site re-oxidation by atmospheric oxygen being faster than the oxidation of CO. From the last column of Table 8, it can be seen that, at a reasonable atmospheric loading of 1 $\mu g/m^3$ for a metal oxide, the half-life of CO is far too long for these processes to contribute to the CO sink. This is true for the stable site process no matter what the value of the re-oxidation rate. The particle loading may actually be higher than this for some metal oxides or the surface area greater, but the conclusion still remains. With the exception of MnO_2 the rate constants or active site concentrations must be in error by more than 10^4 before the effect would be significant in the atmosphere. k_r may have significant errors but not of this magnitude. Kobayashi and Kobayashi's value of k_r for MnO_2 at lower temperatures is 14 times less than our value for the most active site. This lends some credence to our k_r values.

The other mechanisms to test are those involving labile oxygen. Experiments on freshly activated metal oxide with over 200 times the oxygen concentration in each slug as CO are listed in Table 7 and the data presented in Figures 18-21. The data is quite scattered but the effect was in general to increase the CO production by only small factors. The rate would need to increase by at least three orders of magnitude for the labile site or labile O_2 mechanism to be important in the atmosphere. Since the intercepts of the lines in the figures are all less than those without O_2 present, the effect may be interpreted as slow re-oxidation of the stable active sites lost to the depletive mechanism. A steady-state appears to have been reached for MnO_2

Table 8. SLUG REACTOR DATA SUMMARY: RATE CONSTANTS AND CONCENTRATION OF ACTIVE SITES

Metal Oxide	Rate Constant, k_r, cc/mole sec x 10^{-6}, m^3/mole sec.	Active Sites		k_{ar},[b] $m^3/\mu g$ yr.	CO half-li $\tau_{1/2}$, yr.
		A_o, moles/g	A_o, mole sites/mole M_xO_y		
MnO_2	0.52±0.09	6.97×10^{-5}	6.1×10^{-3}	1.1×10^{-3}	606
ZnO	2.5±1.2	3.44×10^{-8}	2.8×10^{-6}	2.7×10^{-6}	2.6×10^{5}
CuO	2.9±0.6	3.82×10^{-8}	3.0×10^{-6}	3.5×10^{-6}	2.0×10^{5}
Fe_2O_3[a]	10.2±0.3	7.48×10^{-9}	1.2×10^{-6}	2.4×10^{-6}	2.9×10^{5}

a. Only two slugs completely depleted maximum loading of sample in the loop, error is range between the two values.

b. k_{ar} is the atmospheric rate constant assuming maximum activity ($k_r A = k_r A_o$).

c. $\tau_{1/2}$ is computed assuming 1 $\mu g/m^3$ atmospheric loading of M_xO_y.

where $dA/dt = 0$. At oxygen concentrations outside the range of the apparatus, this would presumably occur for the other oxides as well. Treating the MnO_2 cata as a steady state of 15 for the slugs where the rate of CO_2 production is constant (see Figure 18) yields a value of $(1.1 \pm 0.4) \times 10^4$ cc mole^{-1} sec^{-1} for k_o ($k_o = K_{(g \rightleftarrows ads)} k_4$).

$$-dA/dt = k_r(CO)(A) - k_o(O_2)(A_o - A) \qquad (15)$$

It would appear that the effect of oxidation by metal oxide particles in the atmosphere on the rate of CO loss from the atmosphere is negligible. This conclusion is based on limited data on only four metal oxides. However, manganese dioxide is known to be one of the more efficient oxidizers of CO at room temperature (due to its large site concentration and not to a high rate constant) and its reaction is too slow to be important by at least three orders of magnitude. One exception possibly exists and that is lead oxide, PbO. We attempted to study this oxide, however, the material could not be rid of labile CO_2 and no quantitative measurements could be made. When slugs of CO were passed through our reactor, no CO effluent could be detected. The capacity to consume CO was great and the k_rA product must be at least that of MnO_2. Lead oxide-carbonate equilibria are known to be facile and one might speculate that a mechanism akin to that observed for NO_2 on metal oxides discussed elsewhere in this document might be operating.

While this work was primarily directed toward atmospheric particle processes, surface reactions at ground level should also occur by similar processes. Hidy[34] has discussed the rate of loss of species at surfaces from a purely mass transport standpoint. Using a global production rate of $\sim 1 \times 10^{12}$ kg/yr of CO[35] and a world land mass area of 5.12×10^{14} m^2, the concentration of CO in the atmosphere is estimated to be 5 ppb using a deposition velocity at 1 cm/sec.[34] and assuming that each collision results in loss of CO from the atmosphere. Since the global CO average is .1 - 2 ppm[35] this calculation only shows that delivery of CO to the earth's surface is not the limiting factor. To check the viability of heterogeneous process occuring on surface layers of soil by purely chemical means, a test calculation was

performed using our rate constants and maximum activities for the four metal oxides under the following assumptions:

1. The average crystal content of the various metals was used in soil with 1 m^2/g[34] surface area and a density of 1.25 g/cc including 50% void volume.
2. The penetration depth of gases into the soil was 2 cm.[36]
3. The composition of the surface of the soil particles is that given in 1 above and 10% of the surface metal concentration exists as the active metal oxide form.

Table 9 shows the results of the computation. The rate constant, k_{sr}, has been converted into units that may be compared with the deposition velocity. Hidy's value for CO of 1 cm/sec translates to 3×10^5 m/yr. compared with the largest rate constant of 59 m/yr. This shows that under the assumptions the chemical process is rate limiting. The rate of CO consumption by these oxidation processes is shown in the last column. The total for the four metals is approximately 1% of the total CO input rate. While this would be a small contributor to the CO sink the inclusion of other metals may well increase this contribution significantly. Of course the assumptions used in the calculation may be overly optimistic and the rate may be very small. In conclusion, further work examining the oxidative abilities of other metal oxides and of natural surfaces are necessary to ascertain the importance of metal oxides as ground level CO sinks.

Table 9. ESTIMATED RATES OF CO OXIDATION BY METAL OXIDES ON SOILS

Metal	Crustal Composition,[a] w/w	A_{os},[b] moles/cc (soil)	K_{sr},[c] m/yr	Rates CO loss[d] kg/yr
Fe	5×10^{-2}	1.7×10^{-12}	21.9	2.5×10^{9}
Mn	1×10^{-3}	9×10^{-11}	59.0	6.9×10^{9}
Zn	1.3×10^{-4}	2.5×10^{-14}	0.079	9.2×10^{7}
Cu	7×10^{-5}	6.7×10^{-14}	0.245	2.9×10^{7}
			Total	9.5×10^{9}

a. Ref. 37

b. Moles of active sites per cc of soil, see text for assumptions.

c. $(2\, k_r\, A_{os}\, d)$, where 2 corrects for the volume occupied by the soil and the d is the depth of the active layer (2 cm).[31]

d. Based on a world land area of 5.12×10^{14} m^2 and 0.2 ppm.

SECTION VII

REFERENCES

1. Ford, H. W. and N. Endow. Rate Constant at Low Concentrations. III. Atomic Oxygen Reaction in the Photolysis of NO_2 at 3660Å. J. Chem. Phys. 27: 1156 - 1160, November 1957.

2. Altshuller, A. P. and J. J. Bufanlini. Photochemical Aspects of Air Pollution: A Review. Photochemistry and Photobiology (London). 4: 97 - 146, 1965. Environ. Sci. Tech. 5: 39 - 64, January 1971.

3. Schuck, E. A. and E. R. Stephens. Oxide of Nitrogen. In: Advances in Environmental Science, Pitts, J. N. and R. L. Metcalf (ed). New York, Wiley-Interscience. 1969. Vol. 1. p. 73 - 118.

4. Judeikis, H. S. and S. Siegel. Particle-Catalyzed Oxidation of Atmospheric Pollutants. Atmospheric Environment. 7: 619 - 631, June 1973.

5. Weinstock, B. and H. Niki. Carbon Monoxide Balance in Nature. Science. 176: 290 - 292, April 1972.

6. Bortner, M. H., R. H. Kummler, and L. S. Jaffe. A Review of Carbon Monoxide Sources, Sinks and Concentrations in the Earth's Atmosphere. General Electric Co. Philadelphia, Pa. NASA CR-2081. National Aeronautics and Space Administration. June 1972. 51p.

8. Nagarjunian, T. S. and J. G. Calvert. The Photooxidation of Carbon Monoxide on Zinc Oxide. J. Phys. Chem. 68: 17 - 26, January 1964.

9. Brooks, C. S. The Kinetics of Hydrogen and Carbon Monoxide Oxidation over a Manganese Oxide. J. Catalysis. 8: 272 - 282, 1967.

10. Kobayashi, M and H. Kobayashi. Application of Transient Response Method to the Study of Heterogeneous Catalysis. I. Nature of Catalytically Active Oxygen on Manganese Dioxide for the Oxidation of Carbon Monoxide at Low Temperatures. J. Catalysis. 27: 100 - 107, October 1972.

11. Kobayashi, M. and H. Kobayashi. Application of Transient Response Method to the Study of Heterogeneous Catalysis. II. Mechanism of Catalytic

Oxidation of Carbon Monoxide on Manganese Dioxide. J. Catalysis. 27: 108 - 113, October 1972.

12. Kobayashi, M. and H. Kobayashi. Application of Transient Response Method to the Study of Heterogeneous Catalysis. III. Simulation of Carbon Monoxide Oxidation Under an Unsteady State. J. Catalysis. 27: 114 - 119, October 1972.

13. Hall, W. K. and P. H. Emmett. An Improved Microcatalytic Reactor. J. Am. Chem. Soc. 79: 2091, 1957.

14. Calvert, J. G. and J. N. Pitts. Effects of Wavelength and Temperature on Primary Processes in the Photolysis of Nitrogen Dioxide and a Spectroscopic Photochemical Determination of the Dissociation Energy. J. Chem. Phys. 42(12): 3655 - 3662, June 1964.

15. Fontijn, A., A. J. Sabadell, and R. J. Ronco. Feasibility Study for the Development of a Multifunctional Emission Detector for Air Pollutants Based on Homogeneous Chemiluminescent Gas Phase Reactions. AeroChem Research Labs, Princeton, N. J. Report Number TP-217. September 1969.

16. Hall, T. C. and F. E. Blacet. Separation of the Absorption Spectrum of NO_2 and N_2O_4 in the Range of 2450 - 5000Å. J. Chem. Phys. 20(11): 1745 - 1749, November 1952.

17. Gelbwachs, J. A., M. Birnbaum, A. W. Tucker, and C. L. Fincher. Fluorescence Determination of Atmospheric NO_2. Opto-electronics (London). 4: 155 - 160, May 1972.

18. Hall, W. K., D. S. MacIver, and H. P. Weber. Semiautomatic Microreactor for Catalytic Research. Inc. Eng. Chem. 52: 421 - 426, May 1960.

19. Stewart, T. B. A Positive Displacement Gas Circulating Pump. Rev. Sci. Inst. 44: 1144, August 1973.

20. Shoemaker, D. P. and C. W. Garland. Experiments in Physical Chemistry. New York, McGraw-Hill, Inc., 1967. p. 262 - 271.

21. Brunaur, S., P. H. Emmett, and Teller. Adsorption of Gases in Multimolecular Layers. J. Am. Chem. Soc. 60: 309 - 319, February 1938.

22. Cheng, R. T., J. O. Frohlinger, and M. Corn. Aerosol Stabilization for Laboratory Studies of Aerosol-Gas Interactions. J. Air Poll. Control Assoc. 21: 138 - 142, March 1971.

23. Judeikis, H. S. and S. Siegel. Efficiency of Gas-Wall Reactions in a Cylindrical Reactor. The Aerospace Corporation. El Segundo, Calif. Report Number ATR-73(7256)-2. 23p. See also Appendix B.

24. Feigl, F. Spot Test in Inorganic Analysis. 5th ed. El Sevier Pub. Co., New York, 1958. p.326 - 332.

25. Muller, P. K., S. Twiss, and G. Sanders. Selection of Filler Media: An Annotated Outline. Air and Industrial Hygiene Laboratory, State of California, Department of Public Health. (Presented at the 13th Conference on Methods in Air Pollution and Industrial Hygiene Studies. Berkeley. October 30-31, 1972) 12p.

26. Calvert, J. G. and J. N. Pitts. The Interaction of Light with Simple Molecules. In: Photochemistry. New York, John Wiley & Sons, Inc., 1966. p.208.

27. Denbigh, K. Tubular Reactors. In: Chemical Reactor Theory. Cambridge, The University Press. 1961. p. 46.

28. Moelwyn-Hughes, E. A. Mathematical Formulation of the Kinetic-Molecular Theory. In: Physical Chemistry. 2nd ed. New York, Pergamon Press. 1961. p.46.

29. Paneth, F. and K. Herzfeld, Z. Elektrochem., 37, 577 (1931).

30. Wise, H. and C. M. Ablow, J. Chem. Phys., 29, 634 (1958).

31. Jost, W. Diffusion in Solids, Liquids, Gases, Academic Press Inc., N. Y., 1960, pp 51-54

32. Carslaw, H. S. and J. C. Jaeger, Conduction of Heat in Solids, 2nd ed, Clarendon Press, Oxford, 1959, pp 188-213.

33. Present, R. D., Kinetic Theory of Gases, McGraw-Hill Book Co., Inc., N. Y., 1958, pp 52-55.

34. Hidy, G. M., Removal Processes of Gaseous and Particulate Pollutants. In: Chemistry of the Lower Atmosphere. ed. by S. I. Rasool. New York, Plenum Press, 1973. pp. 121-173.

35. Jaffe, L. S., Carbon Monoxide in the Biosphere: Sources, Distribution, and Concentrations. J. Geophys. Res. 78: 5293 - 5305, August 1973.

36. Seim, E. C., Sulfur Dioxide Absorption by Soil. Diss. Abs. Intl. B31: 5111-B, 1971.

37. Weast, R. C., ed. , Handbook of Chemistry and Physics, 52 ed. Cleveland, The Chemical Rubber Co, 1971, p F-163.

SECTION VIII
LIST OF INVENTIONS AND PUBLICATIONS

A. Invention:

Stewart, T. B. Positive Displacement Gas Circulating Pump. The Aerospace Corp. Disclosure Number 72-30 'Piston Pump'. Reported separately to E.P.A. on Form 3340.

B. Publications:

1. Judeikis, H. S. and S. Siegel. Particle-Catalyzed Oxidation of Atmospheric Pollutants. Atmospheric Environment (London). 7: 617 - 631, June 1973.
2. Stewart, T. B. Positive Displacement of Gas Circulating Pump. Rev. Sci. Instrum. 44: 1144, August 1973.
3. Judeikis, H. S. and S. Siegel. Efficiency of Gas-Wall Reactions in a Cylindrical Flow Reactor. Submitted to J. Phys. Chem.
4. Hedgpeth, H., S. Siegel, T. Stewart, and H. Judeikis. Cylindrical Flow Reactor for the Study of Heterogeneous Reactions of Possible Importance in Polluted Atmospheres. Submitted to Rev. Sci. Instrum.
5. Badcock, C. C., S. Siegel, T. B. Stewart, and J. K. Allen. On the Possibility of the Heterogeneous Oxidation of CO in the Atmosphere. In preparation.
6. Stewart, T. B. and H. S. Judeikis. Spatial Reactant/Product Concentration in Flow Reactors Using Non-Probe Laser Induced Fluorescence. In preparation.
7. H. S. Judeikis, S. Siegel, T. Stewart, and H. Hedgpeth. The Role of Gas-Solid Interactions in Polluted Atmospheres. II. Reactions of NO_2. In preparation.
8. H. S. Judeikis, S. Siegel, T. Stewart, and H. Hedgpeth. The Role of Gas-Solid Interactions in Polluted Atmospheres. III. Reactions of NO. In preparation.

C. Reports:

1. Judeikis, H. S. and S. Siegel. Particle-Catalyzed Oxidation of Atmospheric Pollutants. The Aerospace Corporation. El Segundo, Calif., Report Number ATR-73(7256)-1, November 1972.
2. Judeikis, H. S. and S. Siegel. Efficiency of Gas-Wall Reactions in a Cylindrical Flow Reactor. The Aerospace Corporation. El Segundo, Calif., Report Number ATR-73(7256)-2, January 1973. 23p.
3. Stewart, T. B. Positive Displacement Gas Circulating Pump. The Aerospace Corporation. El Segundo, Calif., Report Number ATR-73(7256)-3, June 1973. 7p.
4. Hedgpeth, H., S. Siegel, T. Stewart, and H. Judeikis. Cylindrical Flow Reactor for the Study of Heterogeneous Reactions of Possible Importance in Polluted Atmospheres. The Aerospace Corporation. El Segundo, Calif., Report Number ATR-73(7256)-4, August 1973. 21p.

SECTION IX

APPENDIXES

APPENDIX A

MEASUREMENTS OF HOMOGENEOUS AND HETEROGENEOUS REACTION KINETICS OF NO BY OPTICAL ABSORPTION

HOMOGENEOUS GAS PHASE OXIDATION OF NO

Oxidation of NO by O_2 in the gas phase is described by the following relation[3]

$$d[NO_2]/dt = 2k_G [NO]^2[O_2]. \quad (15)$$

In a tubular-flow reactor, such as that described in this paper, the rate of change of $[NO_2]$ with time is related to its rate of change with distance by the expression

$$d[NO_2]/dt = dV/dt \cdot dZ/dV \cdot d[NO_2]/dZ = F/A\, d[NO_2]/dZ \quad (16)$$

where A = the cross sectional area of the tube

F = gas flow rate (cm^3/sec)

Z = length down the tube.

Equation (16) is based on the plug-flow assumption, that is, over any cross section normal to the gas flow, the mass flow rate and gas properties (pressure, temperature, composition) are uniform.[27] By combining Equations (15) and (16), using the material balance relation

$$[NO]_o = [NO] + [NO_2] \quad (17)$$

and integrating, we obtain the following:

$$[NO_2] = [\alpha Z/(1 + \alpha Z)][NO]_o \quad (18)$$

where $[NO_2]$ = the NO_2 concentration down the tube

$\alpha = 2(A/F)\, k_G [O_2][NO]_o$

In deriving Equation (18), we have assumed $[O_2] \approx$ constant since, in our experiments, $[O_2]/[NO]_o \leq 100$ and oxygen is not depleted to any appreciable extent during the course of reaction.

Assuming that the absorption of light by NO_2 in the tubular reactor is described by the Beer-Lambert law,

$$d \log I/dZ = -\epsilon[NO_2] \quad (19)$$

where ϵ = the molar extinction coefficient of NO_2.

[We shall use log for common logarithms (base 10) and ln to designate Naperian logarithms. Also the association reaction $2NO_2 = N_2O_4$ could cause deviations from the Beer-Lambert law. However, in our experiments the pressure of NO_2 was kept sufficiently low so that this association reaction was negligible.] Substitution of Equation (18) into Equation (19) and integration yields the result

$$\log(I_o/I) = \epsilon[NO]_o \ell \left[1 - (1/\alpha\ell)\ln(1 + \alpha\ell)\right] \tag{20}$$

where ℓ = length of the tubular reactor.

Experimental values for I_o/I, $[NO]_o$, $[O_2]$, ℓ, A, and F were substituted into the expression for α and Equation (20). Using the appropriate value for ϵ (Figure 5), the resulting expression was solved iteratively to determine k_G.

CATALYTIC REACTIONS IN THE $NO-O_2-N_2$ SYSTEM

To some extent, catalytic activity in this system could be determined by use of Equation (20). Thus, if catalytic decomposition of product NO_2 (from the homogeneous gas phase oxidation of NO by O_2) occurred, the observed optical density would decrease and solution of Equation (20) would give a smaller effective k_G. Conversely, if NO were catalytically oxidized to NO_2 at the walls, a larger effective value of k_G would be obtained.

Alternatively, let us assume the overall surface reaction (decomposition of NO_2) can be described by a term such as

$$-\varphi_c \, k_c \left(S/V\right)[NO_2] \tag{21}$$

where k_c = the rate of collision of NO_2 molecules with a surface

S = surface

φ_c = the fraction of collision that lead to reaction.

[Term (21) represents a slight modification of the relation given in Reference 28, to include φ_c and V. Note that this form of the equation assumes that the active surface is homogeneously distributed throughout the reactor. This assumption, although an oversimplification, is sufficient for the screening purposes of these experiments.] Adding this term to Equation (1), with

$$k_c = (kT/2\pi M_{NO_2})^{1/2} \tag{22}$$

where k = Boltzman constant

T = absolute temperature

M_{NO_2} = mass of NO_2 molecule.

Proceeding as before, we obtain the following expression

$$\log\left(\frac{I_0}{I}\right) = \varepsilon[NO]_o \ell \left[\left(1 + \beta + \sqrt{\beta^2 + 2\beta}\right) - \frac{1}{\alpha\ell} \ln\left\{\frac{1}{2}\left[1 + \exp(w\ell)\right] - \frac{(1 + \frac{1}{\beta})}{2(1 + \frac{2}{\beta})^{1/2}}\left[1 - \exp(w\ell)\right]\right\}\right] \tag{23}$$

where α = has same meaning as before

$\beta = (1/2\alpha)\varphi_c (A/F) k_c [S]$

$w = 2\alpha\beta(1 + 2/\beta)^{1/2}$.

Given the appropriate values from experimental measurements or the literature for the quantities appearing in these equations, they can be solved iteratively for φ_c.

Alternatively, we may consider the possibility of catalytic oxidation of NO to NO_2 at the surface. In this case, we may substitute the term

$$\varphi'_c k'_c (S/V)[NO] \tag{24}$$

where φ'_c = the fraction of NO-wall collision leading to reaction

$k'_c = (kT/2\pi M_{NO})^{1/2}$,

for Equation (21).

$$\log\left(\frac{I_0}{I}\right) = \varepsilon[NO]_o \ell \left\{1 - \frac{1}{\alpha\ell} \ln\left[1 + \frac{1}{2\beta'}\left(1 - \exp\left|-2\alpha\beta'\ell\right|\right)\right]\right\} \tag{25}$$

where $\beta' = (1/2\alpha)\varphi'_c (A/F) k'_c [S]$.

As in the preceeding case, these equations may be solved iteratively for φ'_c using the appropriate experimental and literature values for the various parameters.

APPENDIX B

GENERAL SOLUTION FOR FLOW, DIFFUSION, AND WALL REACTIONS IN A CYLINDRICAL REACTOR

We consider a system in which the cylindrical walls (but not the ends) of a tubular flow reactor are coated with catalyst. We assume that C, the reacting gas, disappears via a heterogeneous first-order process (adsorption or reaction) that occurs on the walls with an efficiency ϕ. If the reacting gas is introduced into the system as a dilute component in a large concentration of inert gas, we can assume that the total pressure P and therefore D, the diffusion coefficient of C in the mixture, are approximately constant during the course of reaction. Fick's second law of diffusion with an additional term for flow in the direction of the cylinder axis (under steady-state conditions) is[29-31]

$$D\left(\frac{\partial^2 C}{\partial r^2} + \frac{1}{r}\frac{\partial C}{\partial r} + \frac{\partial^2 C}{\partial^2 x}\right) - v_o \frac{\partial C}{\partial x} = 0 \qquad (26)$$

where r and x refer to radial and longitudinal cylindrical coordinates, and v_o is the linear flow rate in the x direction (equal to F/A, the volume flow rate divided by the cross-sectional area of the cylinder).

The following boundary conditions are applicable to the solution of Equation (26) for the case of interest here

$$C(r,\ x = 0) = C_o$$

$$\frac{\partial C}{\partial r}(r = 0,\ x) = 0 \qquad (27)$$

$$D\ \frac{\partial C}{\partial r}(r = R,\ x) = \phi\, k_r C'$$

where C_o is the initial concentration of C, R is the cylinder radius, k_r is the average velocity of the reacting molecule in the radial direction

[$k_r = (kT/2\pi m)^{1/2}$, where k is the Boltzmann constant, T is the absolute temperature, and m is the mass of the reacting gas molecule[28]] and C' is the concentration of C one mean free path away from the wall.

Paneth and Herzfeld[29] and later Wise and Ablow[30] assumed $C(R) \approx C'$ and obtained the solution of Equation (26) on the basis of the boundary conditions in Equations (27). This assumption, however, is valid only for $\phi \ll 1$. In general, $C(R) = (1 - \phi)\, C'$. If we apply this assumption and the boundary condictions in Equations (27), the solution of Equation (26), following the methods described by other workers,[29-32] is

$$\frac{C}{C_o} = \sum_{i=1}^{\infty} \frac{2 J_o\left(\rho_i \frac{r}{R}\right)}{\rho_i (1 + \delta^2 \rho_i^2) J_1(\rho_i)} \left[\exp(\alpha_i x)\right] \tag{28}$$

where

$$\delta = \frac{D}{k_r R} \frac{(1 - \phi)}{\phi} \tag{29}$$

J_o and J_1 are Bessel functions of the first kind, ρ_i is the ith root of the equation

$$J_o(\rho_i) = \delta \rho_i J_1(\rho_i) \tag{30}$$

and

$$\alpha_i = \frac{F}{2AD} - \left[\left(\frac{F}{2AD}\right)^2 + \left(\frac{\rho_1}{R}\right)^2\right]^{1/2} \tag{31}$$

The application of the limiting cases for $\phi \ll 1$ or $\phi = 1$ to Equation (28) gives the results previously preported.[29-31] (Alternatively, the application of these conditions to the boundary conditions in Equations (27) gives the same boundary conditions specified by the previous authors for $\phi \ll 1$ or $\phi = 1$.)

P and D are related by[33]

$$D = \frac{3000kT}{8\pi d^2 P}\left(\frac{\pi kT}{2\mu}\right)^{1/2} \tag{32}$$

where μ is the reduced mass of the reacting and inert gas molecules, and $d = (d_m + d_n)/2$, where d_m and d_n are the molecular diameters of the reacting and inert gas molecules treated as hard spheres. The other terms have the same representation as before.

In some experiments, we determined the average value of the NO_2 concentration at $r \approx 0$ by measuring the decrease in intensity (due to optical absorption by NO_2 at 475 nm) of a narrow beam of light passing through the center of the cylinder. Calculated values corresponding to the average NO_2 concentration at $r = 0$ may be obtained by setting $r = 0$ in Equation (28) and integrating. In the latter case,

$$\left\langle \frac{C}{C_o} \right\rangle_{r=0} = \frac{\int_o^{\ell} \left(\frac{C}{C_o}\right)_{r=0} dx}{\int_o^{\ell} dx} = \sum_{i=1}^{\infty} \frac{2J_o\left(\alpha_i \frac{r}{R}\right) \exp(\alpha_i \ell) - 1}{\alpha_i \ell \rho_i (1 + \delta^2 \rho_i^2) J_1(\rho_i)} \tag{33}$$

where ℓ is the length of the cylinder.

TECHNICAL REPORT DATA
(Please read Instructions on the reverse before completing)

1. REPORT NO.	2.	3. RECIPIENT'S ACCESSION NO.
EPA-650/3-74-007		

4. TITLE AND SUBTITLE	5. REPORT DATE
The Role of Solid Gas Interactions in Air Pollution	August, 1974
	6. PERFORMING ORGANIZATION CODE

7. AUTHOR(S)	8. PERFORMING ORGANIZATION REPORT NO.
S. Siegel, H. S. Judeikis, and C. C. Badcock	ATR-75(7441)-1

9. PERFORMING ORGANIZATION NAME AND ADDRESS	10. PROGRAM ELEMENT NO.
The Aerospace Corporation 2350 E. El Segundo Blvd. El Segundo, California 90245	1AA008
	11. CONTRACT/GRANT NO.
	Grant No. 801340

12. SPONSORING AGENCY NAME AND ADDRESS	13. TYPE OF REPORT AND PERIOD COVERED
Office of Research and Development U. S. Environmental Protection Agency Washington, D. C. 20460	Final Report, 7/1/71-10/31/7
	14. SPONSORING AGENCY CODE

15. SUPPLEMENTARY NOTES

16. ABSTRACT This study was undertaken to evaluate the potential importance of gas-solid interactions in polluted atmospheres. Model calculations that employed collision theory, transition state theory, and data from the catalysis literature were used to determine the conditions under which the heterogeneous processes could compete with homogeneous gas phase reactions known to be important.

Laboratory experiments were conducted with simulated atmospheres to determine whether or not the theoretically derived criteria could be met under ambient conditions. Among the gases studied were NO_2, NO, O_3, and CO. The selection of the solids used in these studies was based on their abundance in polluted atmospheres, as well as on their known catalytic activity.

Evaluation of the experimental results leads us to conclude that heterogeneous decomposition of NO_2 and O_3, as well as heterogeneous oxidation of CO, can be important atmospheric processes. Results from experiments conducted in the presence of moisture indicate that water does not poison catalytic activity. In fact, in the case of NO_2, activity is significantly increased in the presence of moisture.

In contrast to the results for NO_2, O_3, and CO, it was found that heterogeneous processes that involve NO are not likely to compete with gas phase reactions.

17. KEY WORDS AND DOCUMENT ANALYSIS

a. DESCRIPTORS	b. IDENTIFIERS/OPEN ENDED TERMS	c. COSATI Field/Group
Air Pollution Aerosols Chemical Reactions Catalysis	NO, NO_2, O_3, CO	Chemistry Physical Chemistry

18. DISTRIBUTION STATEMENT	19. SECURITY CLASS *(This Report)*	21. NO. OF PAGES
Release Unlimited	Unclassified	84
	20 SECURITY CLASS *(This page)*	22. PRICE
	Unclassified	

EPA Form 2220-1 (9-73)

ENVIRON
Tech
O
Researc

AN EQU